DEVELOPMENT OF ENERGY COMPENSATED GEIGER MULLER DETECTOR

BASED ON THE T2416A CANBERRA CO. GM DETECTOR

By

Omar Mohamed Noor

A Thesis Submitted in Partial Fulfillment
Of the Requirements for the Degree of
Master of Science

in

Faculty of Energy Systems and Nuclear Science Program
University of Ontario Institute of Technology

April, 2013

Abstract

Geiger Muller counters have been a fundamental device in radiation detection for decades due to their simplicity and low cost. Canberra Company has been designing and manufacturing Geiger Muller detectors in various designs for radiation monitoring and field characterization. However, these devices have a draw back when it comes to radiation activity measurements due to the over response of the detector in low energy range i.e., 20 - 250 keV. One of the widely used Geiger Muller counter in the industrial sector is the T2416A. This device is used not only as a survey meter in high intensity gamma radiation fields, but also as a detection device employed in different survey meters for calibration purposes. Among such instruments one can cite the Inspector 1000 and the RadiaGem system. The T2416A GM detector has an over response in the low energy region of about a factor of 6 to 40 relative to ^{137}Cs energy (i.e. 662 keV). In an attempt to flatten this response, in this study, the counter has been redesigned to be an energy compensated Geiger Muller counter. To achieve this goal, a special filtering material has been designed with a composition of different materials and in different thicknesses. The work has been carried out by adopting an approach of simulating the response of the detector with different materials as well as measurements at different photon energies up to 250 keV with and without filtering materials. A series of experimental and simulation data has been analyzed and compared against each other.

Acknowledgment

I would like to express my ultimate and sincere gratitude to GOD, Almighty, for His blessings and support. I am indeed grateful to my family but especially to my wife, Melissa Girard, for her continued love and support throughout our marriage particularly during the course of my studies.

I am greatly in debt to Dr. Machrafi, who engraved in me the sense of creativity, leadership and the love of research. In addition, I would like to thank my professors at UOIT, especially A. Waker, Ed. Waller for their support.

During my time at Canberra, I have received support from the Canberra team and I am truly grateful to all of them especially R. Watson, F. Finelli, and G. Bogorodzki. Last but not least, I would like to thank the committee members - Dr. M. Kaye, Dr. A. Waker, and Dr. G. Orchard - for enriching the thesis with their constructive comments.

Table of Contents

List of Figures

Chapter 1: **Introduction**

The discovery of the existence of radiation was a turning point in the history of humanity. Whether by accident or not, the honour of such a discovery is attributed to Wilhelm Roentgen in 1895. Roentgen not only discovered radiation in the form of X-rays but also discovered a method of detecting radiation. Many of the advantages we enjoy in life are associated with the discovery of radiation. Some of the many beneficial applications that have evolved from the discovery of radiation are: electricity production via nuclear power plants, medical diagnosing of diseases through various radiation-based imaging techniques, and the source of cure of some diseases through the use of high energy X-rays, gamma rays, electrons or particles beams in radiotherapy.

Just as with any other invention or discovery, there are some disadvantages associated with the use of nuclear/radiation-based technologies. The greatest disadvantage is the fact that radiation cannot be sensed by our five senses hence raise the need to use a tool to detect radiation in order to control and monitor radiation which is known to damage biological materials and organisms. Radiation can be a great source of threat to our health, life and the environment if not properly monitored and controlled. This has led the nuclear industry to place a great emphasis on the development of radiation detectors that are able to detect different types of radiation and provide accurate and reliable information about the nature of existing radiation and its possible hazard.

The oldest and yet most commonly used radiation detector today is the Geiger Muller (GM) counter. Hans Geiger and Walther Muller invented GM detectors in 1908 [1]. Though

GM detectors are one of the oldest detectors, they are still widely spread and used in the nuclear industry and that is due to their simplicity and low cost [2]. A GM detector is mainly a cylindrical tube with an inner wall that acts as a cathode and a thin wire running along the axis of the tube that acts as an anode with a high potential difference between the two electrodes.

The initial GM detector went through various stages of development and improvement. Some of the major improvements include the development that was introduced in 1937 by Adolf Trost, who addressed the problem with the re-triggered pulses following a Geiger discharge. These re-triggered pulses are caused by electrons ejected from the cathode wall as a result of the interaction of the positive ions with the atoms of the cathode wall. The proposed solution was the addition of a secondary element to the filling gas, known as the quenching *gas*. The quenching gas suggested by Trost was ethanol [1]. The main purpose of the quenching gas is to neutralize the positive ions produced by the ionization particle through the transfer of electrons from the quenching gas to the positive ion. The positive ions of the quenching gas break apart once they collide with the wall of the detector without producing any electrons. The quenching gas is eventually eliminated as a result of its breaking apart after every Geiger discharge, which puts a lifetime limitation on the GM tube. The problem of lifetime limitation due to the type of quenching gas used was later addressed in 1938 by S. H. Liebson and H. Friedman, who suggested the use of an inorganic halogen quenching gas instead of an organic quenching gas. The main advantage of using an inorganic halogen gas is its ability to recombine following its breaking apart [1]. The usage of such gases removes any limitation with regard to the lifetime of the GM tube.

GM detectors suffer from a problem related to their response function to gamma rays with various energies, especially in the low energy region of gamma radiation. The response of the GM detector is basically energy dependent i.e. measured activity is dependent on the energy of the source. Gamma rays with low energies produce higher counts than gamma rays with higher energies. Some research has been conducted to address such a problem. Before commenting on some of the work completed on this issue, it is useful to reflect on the seriousness of this problem. A GM detector is known as a counter, it counts single events, i.e. operation in pulse mode and acting as a counter. GM detectors are unable to provide information related to the energy of the incident radiation. A GM detector that is energy dependent may provide inaccurate counts of present radiation. This problem puts the reliability of GM detector into question, especially when it is widely used in large radiation monitors for calibration purposes. Therefore international regulatory organizations have placed strict rules regarding the production of GM detectors with an improved response that is somewhat independent of the incident gamma energies [17].

In 1964, Danchenkot and Mitrofanov, studied the GM energy dependence issue. They focused on the response of the GM detector for gamma rays with an energy range of 0.5 to 1.4 MeV. They found that the GM detector has a higher response to gamma rays with energies above 1 MeV relative to Cs-137. In their analysis, they determined that gamma rays with energies higher than 1.022 MeV interact via pair production which has a probability of interaction that is mainly proportional to the atomic number to the power of 2, Z^2 [3]. To minimize the over response of the GM detector for this range they suggested the wall of the detector to be constructed from a material with a low Z value, such as beryllium [1].

On the other hand, Centronic, a leading manufacturer of radiation detectors, studied the over response of the GM detector to low energy gamma rays in reference to Cs-137. In 1986, they developed four types of GM detectors with an improved response function which was achieved by adding shielding material that were either made of copper, lead, tin or a combination of both of tin and lead. For the four types of detectors, a two-component filter with a central gap was used [4]. The shielding material basically attenuate gamma rays with low energies hence, limiting their counts.

There are few companies around the world that produce energy compensated GM detectors. Canberra Co., which is an Areva company, has taken the initiative to produce an energy compensated GM detector out of the T2416A GM detector to meet the demand of the local and international market. Based on their request a collaboration project with University of Ontario Institute of Technology (UOIT) was initiated in early 2011 with the main objective of investigating the possibility of locally manufacturing an energy compensated GM detector based on their widely used T2416A GM detector that over responds to gamma rays with low energies; i.e. from around 20 keV to 250 keV.

The main objective of this research is to investigate the impact of various design features in lowering the response of the T2416A GM detector to gamma rays with an energy range of 20 to 250 keV. By lowering the response of T2416A, it would then be considered an energy compensated GM detector. The following design features were selected for this research work;

1) Different mechanism for wrapping the filtering material around the GM which include

   a) One-Piece Wrapping Model

b) Two-Piece Wrapping Model

2) Determining the appropriate filtering material which includes:

a) A Single filtering material

b) A combination of filtering materials with different weight percentages

To achieve the cited objectives, a combined methodology of simulation, using MNCNP/X, along with a series of experiments carried out at the Canberra site was adopted. This research mainly depends on the simulation data obtained using MCNP/X. Results obtained from the simulation data have been compared to the available experimental data. Based on the results obtained from the above investigations an energy compensated GM detector was developed.

The thesis consists of four chapters, a conclusion, and future work, and concludes with a list of references and appendices. Current chapter consists of the general background of the history of GM detectors and presents a literature review of some of the completed work on the improvements of GM detectors to date. Chapter two provides a description of sources, interactions and detection of gamma rays with an emphasis on the GM detector. Chapter three covers the methodology used in this research to achieve the above listed objectives. Details are provided about the MCNP/X code used to simulate the response of the GM detector to low energy gamma rays. Chapter four presents the results obtained from the simulation work with a comparison against experimental results. The impact of each of the parameters listed above on the response function of the GM detector is also discussed in this chapter. Based on the discussion related to the obtained results, conclusions have been drawn to summarise the impact of each of the design features in

lowering the response of the T2416A GM detectors to gamma rays with low energies. The thesis concludes with a list of references and a brief description of suggested future work.

Chapter 2: **Gamma-ray Interaction and Detection**

In this chapter, the nature of gamma rays is highlighted along with the various sources through which gamma rays are produced. Once the sources of gamma rays are highlighted, then their mode of interactions is discussed. There are three main modes of gamma interaction. These modes of interactions are the foundation of the gamma ray detection. There are various types of detectors that are discussed in this chapter. A great emphasis is put toward GM detectors and their operation, components and response to gamma rays.

2.1 Photon Sources

Gamma and X-rays are electromagnetic radiation that have a mass and a charge of zero. Due to their lack of charge and mass, gamma and X-rays have a very strong penetration power. The main difference between gamma rays and X-rays is their source of origin. Gamma rays are emitted from the nuclei of the atom as a result of a rearrangement of protons/neutrons, whereas X-rays are emitted from the atom as a result of the rearrangement of orbital electrons. There are several sources whereby a gamma ray may be obtained. In this chapter, these sources are discussed in detail [2].

2.1.1 Gamma ray following Beta Decay

For an unstable atom that has a high neutron-to-proton ratio such as Po-210, stability is achieved though the transforms of a neutron to a proton and an electron [3]. The electron (beta particle) is ejected and hence this type of decay is known as beta decay. The daughter of the decayed atom is left in an excited state therefore a gamma ray is emitted to de-excite the atom. The energy of the emitted gamma ray is a characteristic of the daughter atom since it reflects the energy level structure of the daughter nucleus. However, the gamma

ray appears with the half-life of the parent [2]. For instance Cs-137 decays through beta minus decay to Ba-137 which is in an excited state. Ba-137 de-excites through emitting a gamma ray with energy equal to 662 keV. The emitted gamma ray is emitted according to the Cs-137, the parent, half-life which is 30 years. Figure 1 illustrates the decay scheme of Cs-137 described above.

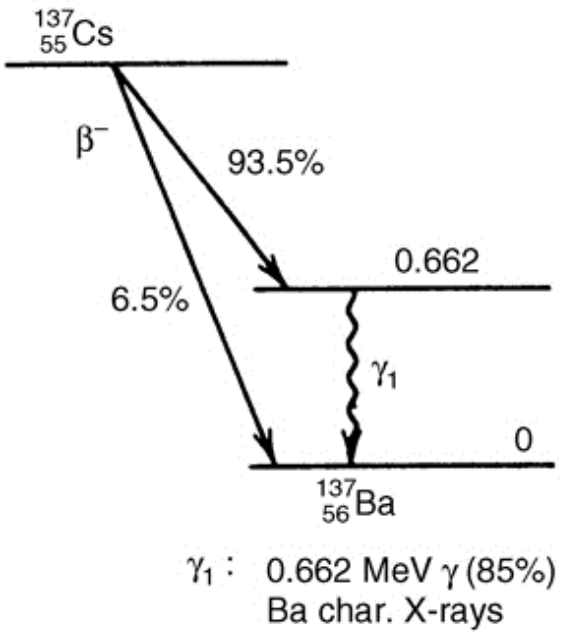

Figure 1: Decay Scheme for ^{137}Cs [2]

2.1.2 Annihilation Radiation

Annihilation radiation is generally associated with the vanishing of a positron particle. A positron is identical to an electron in all aspects except its charge, it is positively charged. A positron is produced through a beta positive decay whereby an atom with a low neutron-to-proton ratio may decay through a positron emission [3]. Pair production interaction of a gamma ray with a high energy may also produce a positron. In either case, due to the

nature of a positron, the positron is destined to vanish. The emitted positron expends all of its kinetic energy through collisions in the matter causing numerous ionization and excitation [5]. At the end of the positron track, the positron combines with an electron in a process known as annihilation. As a result of the annihilation process two gamma rays are emitted in opposite directions. Each gamma ray has an energy equivalent to the rest mass of the electron, 0.511 MeV. Since the positron expends its energy in a very rapid way, the annihilation radiation emission is in virtual coincidence with the original beta positive decay or the pair production interaction [2].

2.1.3 Gama ray following Nuclear Reactions

A radioactive isotope with a low neutron-to-proton ratio tends to decay via alpha emission. Mixing such a radioactive isotope with an appropriate element, such as C-13 or Be-9, results in a nuclear reaction that produces an element in an excited state [2]. The excited product of this nuclear reaction de-excites itself through the emission of a gamma ray. An example of such a reaction is the interaction of americium-241 with beryllium-9. Americium-241 is an alpha emitter. The emitted alpha undergoes a nuclear reaction with beryllium-9 producing a neutron and a carbon-12 atom where the latter is in an excited state. Carbon-12 de-excite through the release of a gamma ray [2].

$$ {}^{4}_{2}\alpha + {}^{9}_{4}Be \rightarrow {}^{12}_{6}C^{*} + {}^{1}_{0}n $$

The nuclear interaction of a thermal neutron through the absorption of typical nuclei may lead to the production of a gamma ray. Such a nuclear reaction is known as an n-γ reaction. There are various sources of neutrons that can be utilized to induce this reaction such as; nuclear reactors, accelerators or radioisotopes of neutron sources [2] [3].

2.1.4 Bremsstrahlung

When a charged particle accelerates or decelerates, an electromagnetic radiation known as *bremsstrahlung* is produced. The acceleration or deceleration is due to the interaction of the incoming charge particle with the electric field due to a similar or an opposite charge [2]. The intensity of the electromagnetic radiation produced is directly proportional to the square of the atomic number and inversely proportional to the square of the mass of the charged particle. Electrons have an insignificant mass thousands times less than the mass of the proton; hence the amount of bremsstrahlung produced by protons is very insignificant in comparison to electrons [2]. The fraction of electrons energy that is converted into bremsstrahlung is also proportional to the energy of the electron. Equation 2.1 is used to calculate the fraction of the electron's energy that is converted into bremsstrahlung.

$$f_\beta = 3.5 \times 10^{-4} Z E_m \qquad 2.1$$

where f_β represents the fraction of the incident beta energy converted into photon, E_m represents the maximum energy of the beta particle in MeV and Z is the atomic mass of the target material [3]. Figure 2 illustrates an incident electron passing though the electric field due to the nuclei and thus is accelerated and in the process a bremsstrahlung radiation is produced.

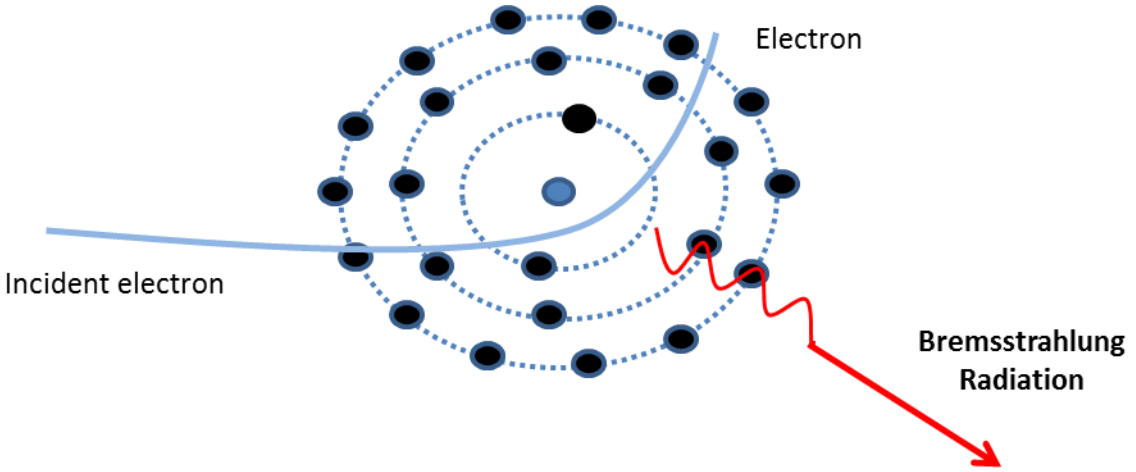

Figure 2: Bremsstrahlung Production

An X-ray machine produces X-rays via this method. Electrons are accelerated in an X-ray tube through the supply of a very high voltage. The accelerated electrons are directed onto a metal target. As a result of the interaction of the electrons with the target, electrons decelerate and slow down and as a result a spectrum of continuous bremsstrahlung radiations are produced. Sharp peaks may exist in this continuous spectrum. These sharp peaks are known as characteristic X-rays which is explained in detail in the following section. A filtering material is added to eliminate or reduce undesired energies of the emitted X-rays.

2.1.5 Characteristic X-rays

A characteristic X-ray is a fingerprint property for each atom; hence it is used in the X-ray fluorescence technique to perform elemental/chemical analysis [6]. A characteristic X-ray is emitted when the electrons in an atom make a transition from a high energy shell to a lower energy shell. The transition of electrons is due to the creation of a vacancy in the

orbital shells of the atom. A vacancy is created as a result of radioactive decay process or due to excitation by external radiation. Thus when an electron jumps from the L shell to the K shell, the characteristic X-ray that is emitted is known as K_α. If the electron jumps from the M shell to the K shell, the characteristic X-ray that is emitted is known as K_β. Figure 3 illustrates a typical X-ray spectrum which consists of a continuous background of bremsstrahlung radiation with a K_α and K_β characteristic X-ray [2].

The energy of the characteristic X-ray that is emitted is equivalent to the energy difference between the two orbital shells. A characteristic X-ray would have maximum energy when the transition takes place from an unbound electron to the K shell [7] [6].

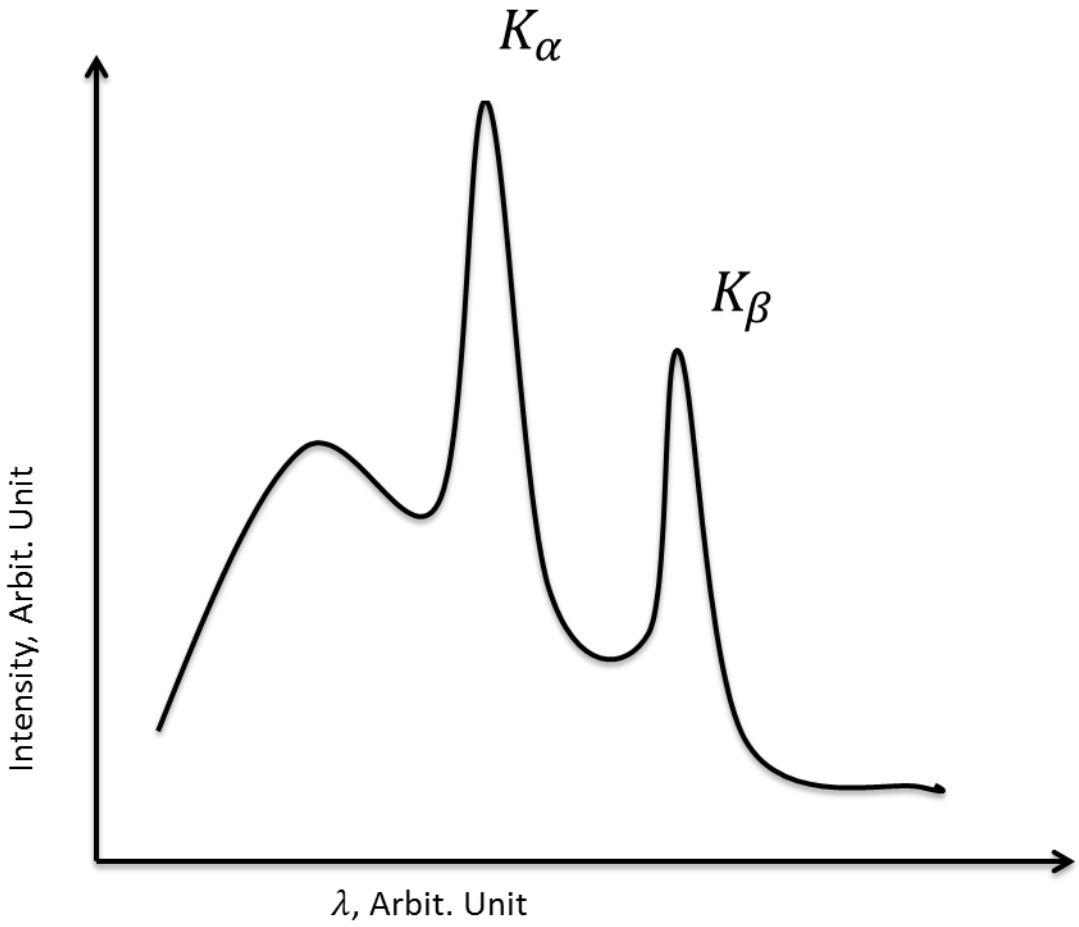

Figure 3: Typical X-ray Spectrum

2.2 Gamma Interaction

X- and Gamma rays are electromagnetic radiation that have a high frequency and high energy. The mass and the charge of a gamma ray are zero. Due to the nature of their charge, x and gamma rays do not interact with charged particles in an atom through an electrostatic force leading to the ionization or the excitation of atom, hence they are known as an *indirect ionizing radiation* [2]. However, they interact mainly through collisions with the electrons in the atom or by interacting with the electromagnetic field due to the presence of charges particles in the atom.

When an incident photon collides with an electron in the atom, the photon either transfers all or part of its energy to the electron. If all of the photon's energy is transferred then the process is knows as *photoelectric effect*. However, if there is only a partial transfer of the incident photon's energy, then the process is known as *Compton scattering*. In either case, an electron is ejected, leading to the ionization of the medium. If the incident photon has energy that is greater than 1,022 MeV then the possibility of colliding with an electron is very slim. Such photons interact with the electric field of the nucleus and, as a result, the photon disappears and an electron and a positron are formed. These three modes of interactions are explained in further detail in this chapter.

Other than the energy of the photon, the Z value of the absorber atom has a great influence in determining which of the above three interactions take place. Figure 4 illustrates regions where each of the above mentioned modes of interactions are dominant with reference to the Z value of the target as a function of gamma energy.

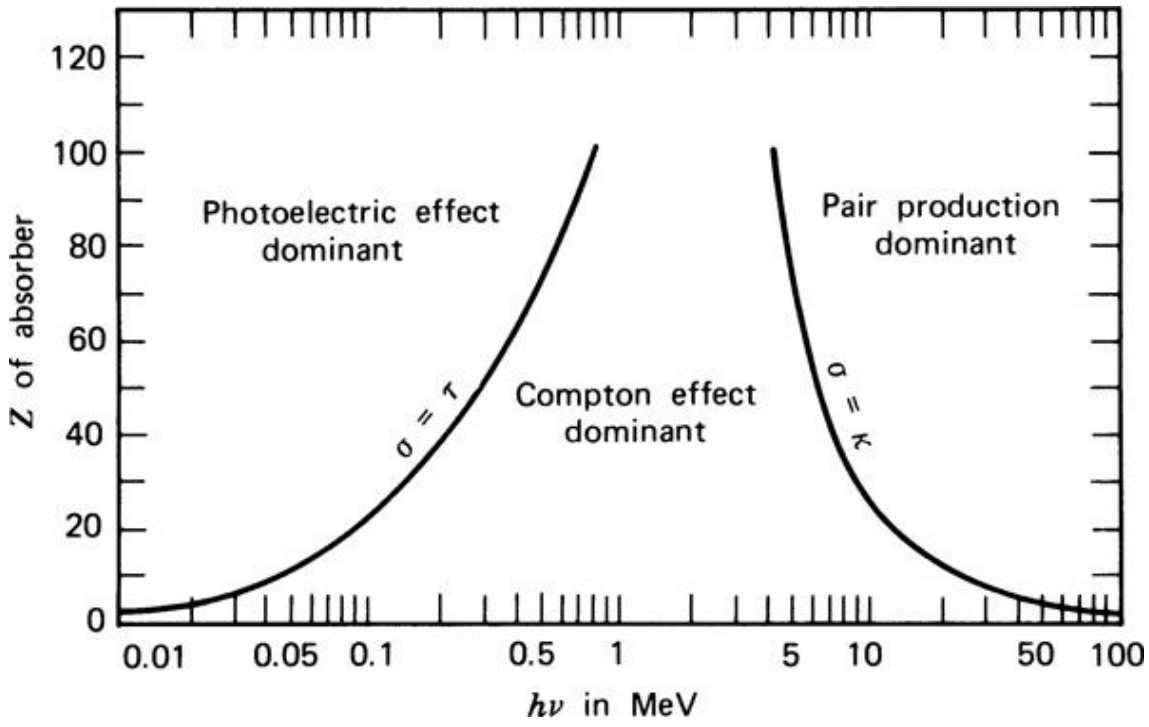

Figure 4: Z/ E Influence on Gamma ray Mode of Interaction [2]

Through observing Figure 4, it can be seen that the *photoelectric effect* is dominant when the photon's energy is low, lower than 0.5 MeV and the Z value of the absorber is high. The Compton scattering, on the other hand, is dominant when the photon's energy is between 0.5 and 1 MeV and the Z value is low. The interaction of photons with the electric field due to the nucleus requires an energy that is higher than 1.022 MeV, which makes this type of interaction dominant when the photon's energy and the Z value are high i.e. E> 10 MeV and Z>40.

2.21 Photoelectric Absorption

An incident photon interacts with the orbital electrons in the absorbing material atom. This interaction takes place with one of the tightly bound electrons. The photon transfers all of its energy to the electron and disappears. If the energy of the incident photon is greater than the binding energy of the electron, then photoelectron is ejected with an energy equivalent to the difference between the incident photon and the binding energy of the electron. The energy of the ejected photoelectron can be determined by using Equation 2.2.

$$E_{e^-} = h\upsilon - E_b \qquad 2.2$$

where E_b represents the binding energy of the electron and h represents Planck's constant and υ represents the wavelength of the photon [2]. The binding energy for electrons in the K shell for materials with a low Z are few keV in magnitude while materials with a high Z value are tens of keV in magnitude [7]. The ejected photoelectron is mostly from the K shell. Once the photoelectron is ejected a vacancy is created in the K shell. An electron from the outer shells fills this vacancy and in the process a characteristic X-ray is emitted or the atom captures an electron from the medium. In most cases the emitted X-ray interacts through photoelectric absorption with an electron that is in a less tightly bound shell.

The probability of photoelectric effect interaction mainly depends on the energy of the incident gamma, the atomic number of the target atom and the binding energy of the electron [2]. The higher the atomic number, the higher is the electron density and hence the higher the probability of photoelectric interaction. On the other hand, the higher the

energy of the incident photon, the lower is the probability of photoelectric interaction [3]. The greater the binding energy or the more tightly bound the electron; the higher is the probability of interaction. Electrons on the K-shell are tightly bounded electrons, which is why 80% of the interactions involve K electrons [7]. The probability of interaction is determined using Equation 2.3.

$$\tau = constant \times \frac{z^n}{E_\gamma^{3.5}} \qquad 2.3$$

The exponent n has a value between 4 and 5; hence the Z value plays a significant role in the probability of interaction which makes elements with high Z values, such as Pb-208 and U-238, a great choice for shielding gamma rays [3]. Figure 5 shows the mechanism of interaction for photoelectric absorption.

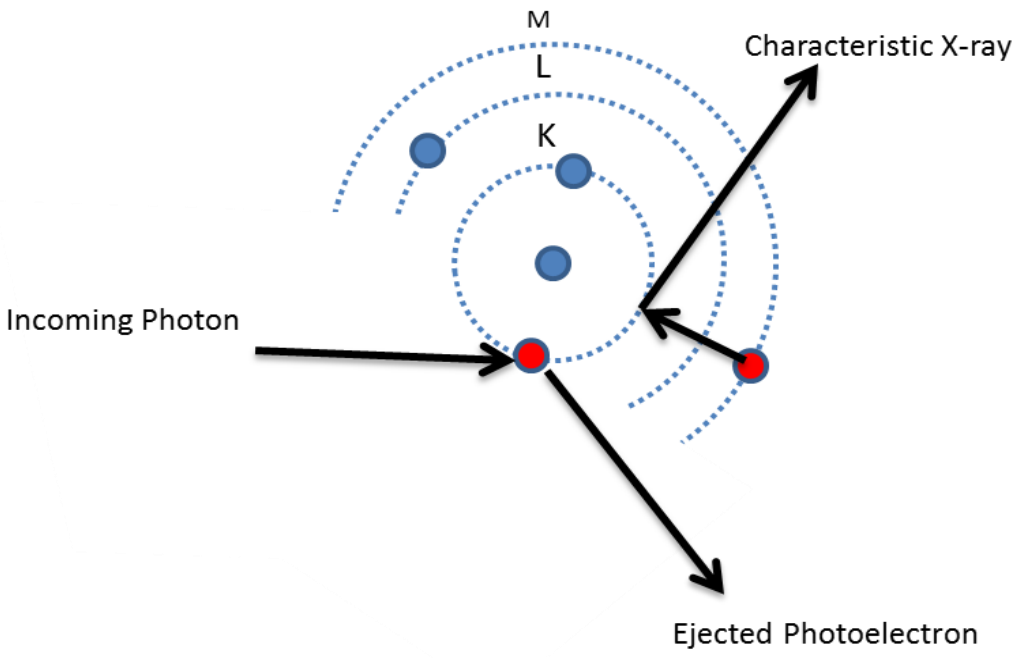

Figure 5: **Photoelectric Effect**

2.2.2 Compton Scattering

In this mode of interaction, an incident photon collides with the absorbing material atom's free electrons, whose binding energy is very small in comparison to the energy of the incident photon. As a result of the interaction the photon scatters and a portion of its energy is transferred to the electron causing the electron to be ejected from the atom. The photon deflects at an angle θ with an energy that is less than the energy of the incident photon as illustrated in Figure 6.

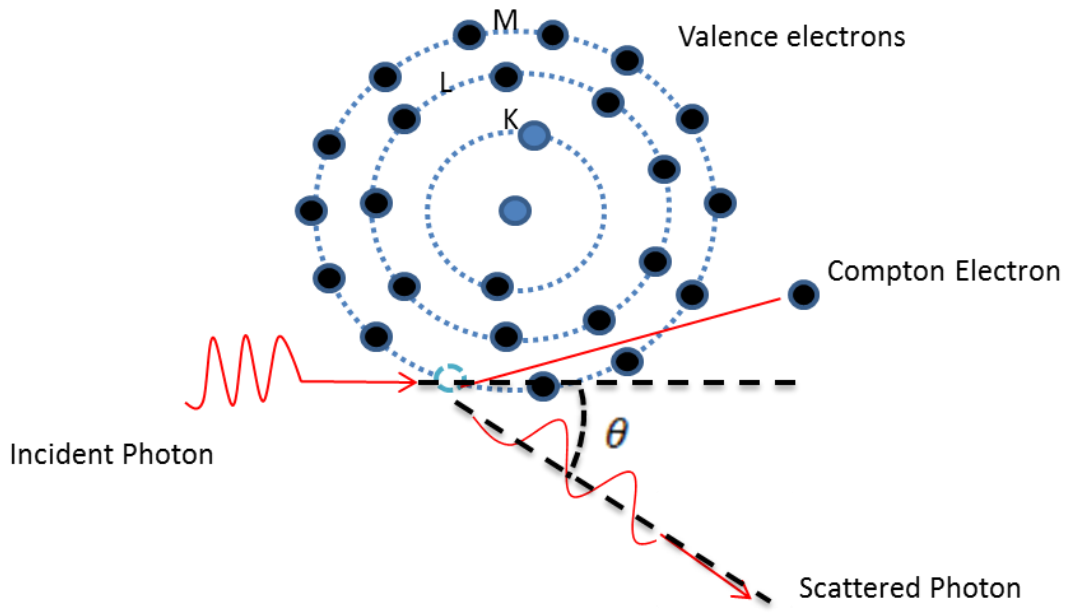

Figure 6: Compton Scattering Interaction

The angle θ can have any value between $0°$ and 180°. The deflected photon have a minimum and a maximum energy when θ is 180° and $0°$, respectively. Equation 2.4 is used to calculate the energy of the ejected electron.

$$E_e = hv - hv' \tag{2.4}$$

hv represents the energy of the incident photon and hv' represents the energy of the deflected photon. Since both of the energy and the momentum have to be conserved, then the energy of the deflected photon is calculated using the following equation [2].

$$hv' = \frac{hv}{1+\frac{hv}{m_0c^2}(1-cos\theta)} \tag{2.5}$$

where m_0c^2 represents the rest mass energy of the electron (0.511 MeV) and θ is the angle of deflection of the photon.

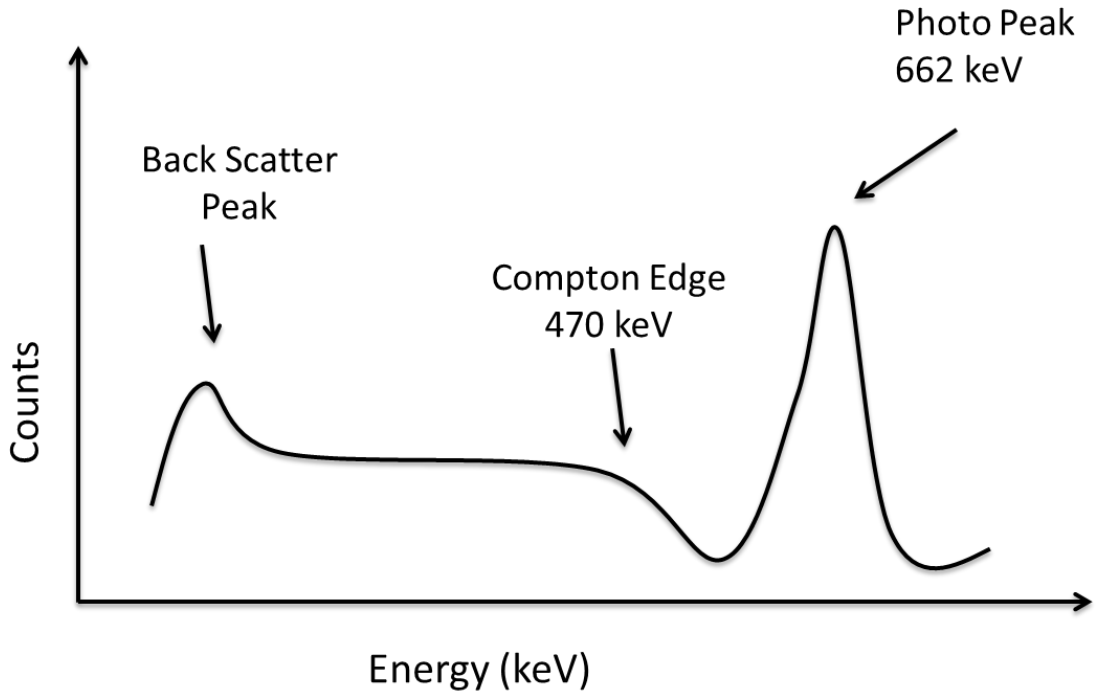

Figure 7: Electron Energy Distribution for 137Cs

Figure 7 shows the electron energy distribution for Cs-137 versus counts measured with a gamma ray NaI scintillator spectrometer. The Compton continuum represents the continuum of energies transferred to the electron due to the variation of scattering angles from $0°$ and180°. The Compton edge shown in Figure 7 represents the maximum energy that can be transferred to the electron. In the case of a 662 keV Cesium source the Compton edge is around 470 keV; this value is calculated using Equation 2.6 [2].

$$E_{e^-} = E\left(\frac{\frac{2E}{m_0c^2}}{1+\frac{2E}{m_0c^2}}\right) \qquad 2.6$$

The gap between the Compton edge and the photo peak is due to the difference between the value of the incident photon and the Compton edge value [2].

The probability of Compton scattering interaction is dependent on the energy of the incident photon and on the electron density of the medium. The electron density is proportional to Z/A which is almost constant for all materials, hence there is less dependency on the medium material. Equation 2.7 is used to determine the probability of interaction for Compton scattering interactions [3].

$$\tau = \frac{Z}{E} \qquad (2.7)$$

where τ is the probability of interaction, Z is the atomic mass number of the absorbing material and E is the gamma ray energy.

2.2.3 Pair Production

In contrast to the first two modes of gamma interaction, this mode does not involve collision with electrons. An incident photon passes through the electric field near the nucleus and as a result the gamma disappears and an electron-positron pair is formed. This materialization is only possible if the incident gamma ray has energy equal to twice the rest mass energy of an electron, 1.02 MeV. If the gamma energy exceeds the threshold energy for this interaction, then the excess energy is shared between the positron and the electron. The above interaction can also take place when an energetic photon passes by an electron. However, the probability of this interaction is very low [3] [5].

The electron and positron produced as a result of this interaction slows down rapidly in the absorbing material. Once, the positron loses most of its kinetic energy it goes through annihilation process, in which a positron combines with an electron and as a result two gamma rays with energy of 0.511 keV each are emitted in opposite directions. These two low-energy gamma rays either both escape the detector region, both deposit their energy in the detector or one escapes and one deposits its energy in the detector [2]. If the energy of both gamma rays is deposited in the detector, then the total energy deposited is equal to the energy of the incident gamma ray. Whereas if any or both of gamma rays escape the detector region then the interaction contributes to the escape peak below the full energy peak [2].

Though the threshold of pair production interaction is 1.022 MeV, the probability of interaction is very low around 1.022 MeV and the probability slowly increases until the photon energy reaches 5 MeV. For example a photon with energy of 1.5 and 2 MeV have

a 20% and 50% rate of pair production respectively when interacting with lead [7]. If the energy of the photon exceeds 5 MeV, the probability of interaction is proportional to the logarithm of the quantum energy. Such an increase leads to an increase of the attenuation coefficient for high energy photons [3]. Figure 8 illustrates the mechanism of pair production interaction.

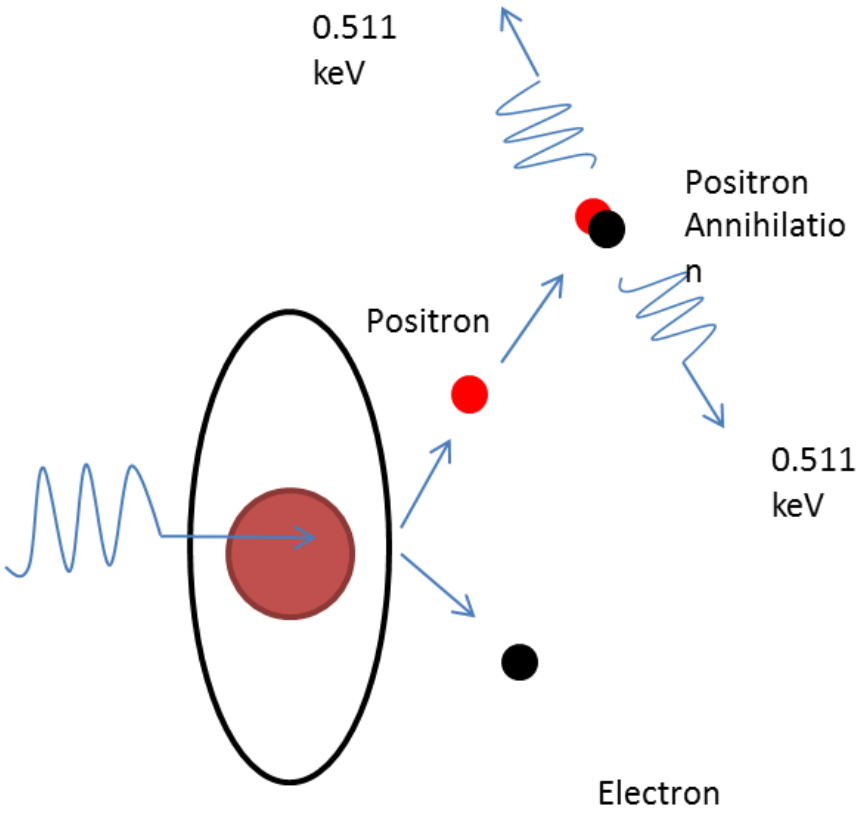

Figure 8: Pair Production

2.3 Gamma ray Attenuation

As a beam of gamma ray traverse any medium, a gamma ray may interact with the atoms of the medium through absorption or scattering. In either case, the photon will end up

being removed from the beam. The probability of photon removal is known as the *linear attenuation coefficient, μ,* which is defined as: the probability per unit path length that the gamma-ray photon is removed from the beam [2]. Every method of gamma ray interaction has its own μ value. The total linear attenuation coefficient can be calculated by adding the μ value for all possible interaction mechanism. Equation 2.8 is used to calculate the total μ value.

$$\mu = \mu_{photoelectric} + \sigma_{compton} + \kappa_{pair\ production} \tag{2.8}$$

μ may also be calculated using the mean free path value, λ. The mean free path is defined as the average path travelled by the incident gamma in a medium without interaction. Equation 2.9 is used to calculate the μ from the mean free path value:

$$\mu = \frac{1}{\lambda} \tag{2.9}$$

Using the μ value, the number of transmitted gamma is calculated using Equation 2.10 where I represents the number of transmitted gamma, I_0 represents the initial number of gamma rays before entering the medium and t is the thickness of the medium.

$$I = I_0\, e^{-\mu t} \tag{2.10}$$

The linear attenuation coefficient values for the same material can vary, based on the density of the material. To avoid such dependency, a mass attenuation coefficient is used instead with a value of linear attenuation coefficient divided by the density of the material.

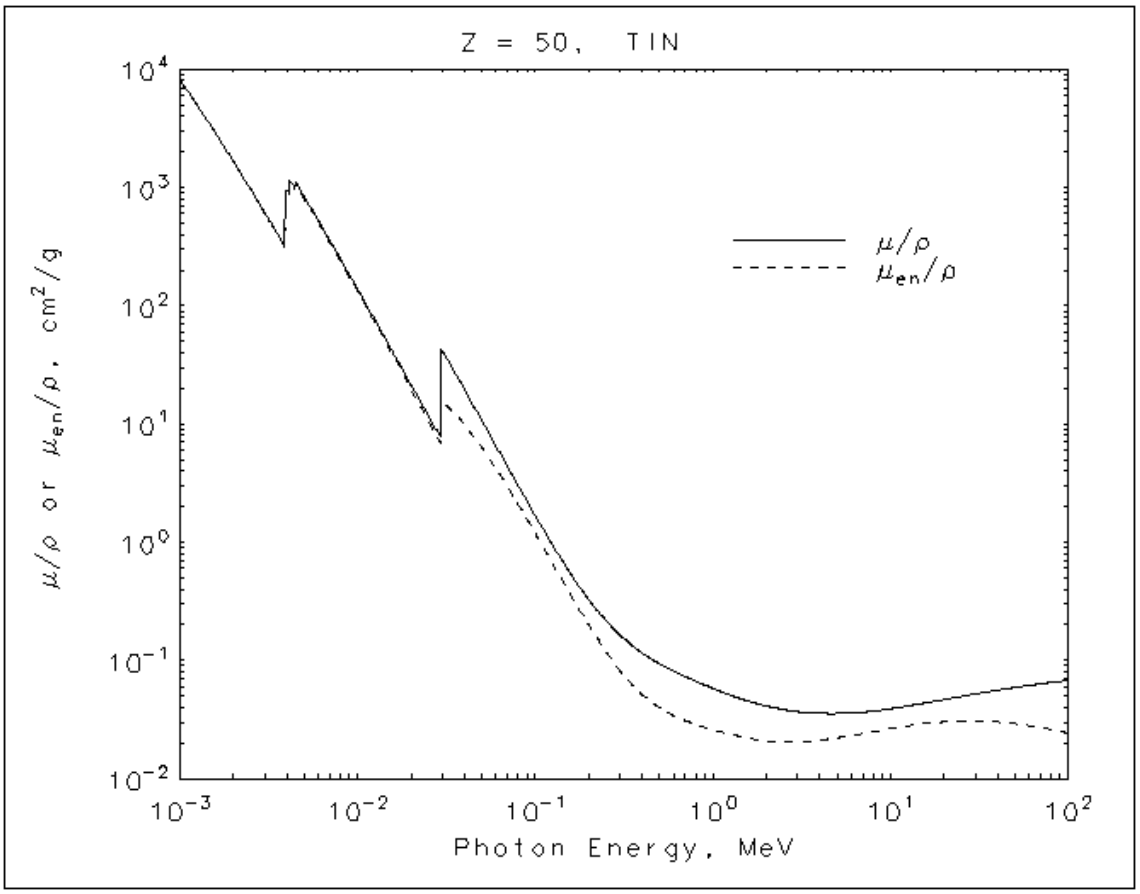

Figure 9: Tin Mass Attenuation Coefficient [2]

Figure 9 represents the mass attenuation coefficient for tin as a function of photon energy. The shape of the curve is dependent on the photon energy and the atomic number of the medium. All mass attenuation coefficient curves follow the same trend as the curve above. At low energy the mass attenuation coefficient or the probability of interaction is high and it smoothly decreases as energy increases. This smooth decrease in mass attenuation is interrupted by peaks were the value of mass attenuation coefficient increases and then decreases again [7]. This increase is due to the absorption edge of various shells. The absorption edge represents the minimum energy needed to eject an electron from a specific

shell. For instance, the minimum energy needed to eject an electron from the K shell in Al and Cu atoms is 1.55 and 8.97 keV, respectively [7]. Further discussion on absorption edges is presented in the next chapter as this concept is strongly related to the fulfilment of the objectives for this thesis.

2.4 Gamma Detectors

There are many types of gamma detectors with various capabilities. Some detectors function just as a counter, while others are able to function as spectrometers. All gamma ray detectors function on the basis of ionization and/or excitation. The incoming gamma ray ionizes the sensitive part of the detector and thus producing electrons and positive ions. The collection and the processing of these ejected electrons reveal the intensity and the energy of the incident gamma ray. In this section the three main types of gamma detectors are discussed in detail.

2.4.1 Scintillation Detectors

As the name implies, these detectors contain a scintillation material. This scintillation material can be solid, liquid or gas and can be organic or inorganic [8]. In either case, the scintillation material emits light as a result of interaction with ionizing radiation. The quantity of the emitted light is proportional to the energy of the ionizing radiation absorbed in the scintillator. Some of the common inorganic scintillation materials are zinc sulfide (ZnS), lithium iodide (LiI), sodium iodide (NaI) and cesium iodide (CsI). The latter two materials are the most commonly used [9]. A good scintillation material must be transparent, large in size “for better sensitivity”, able to produce a large light output that is proportional to the incident gamma energy [10].

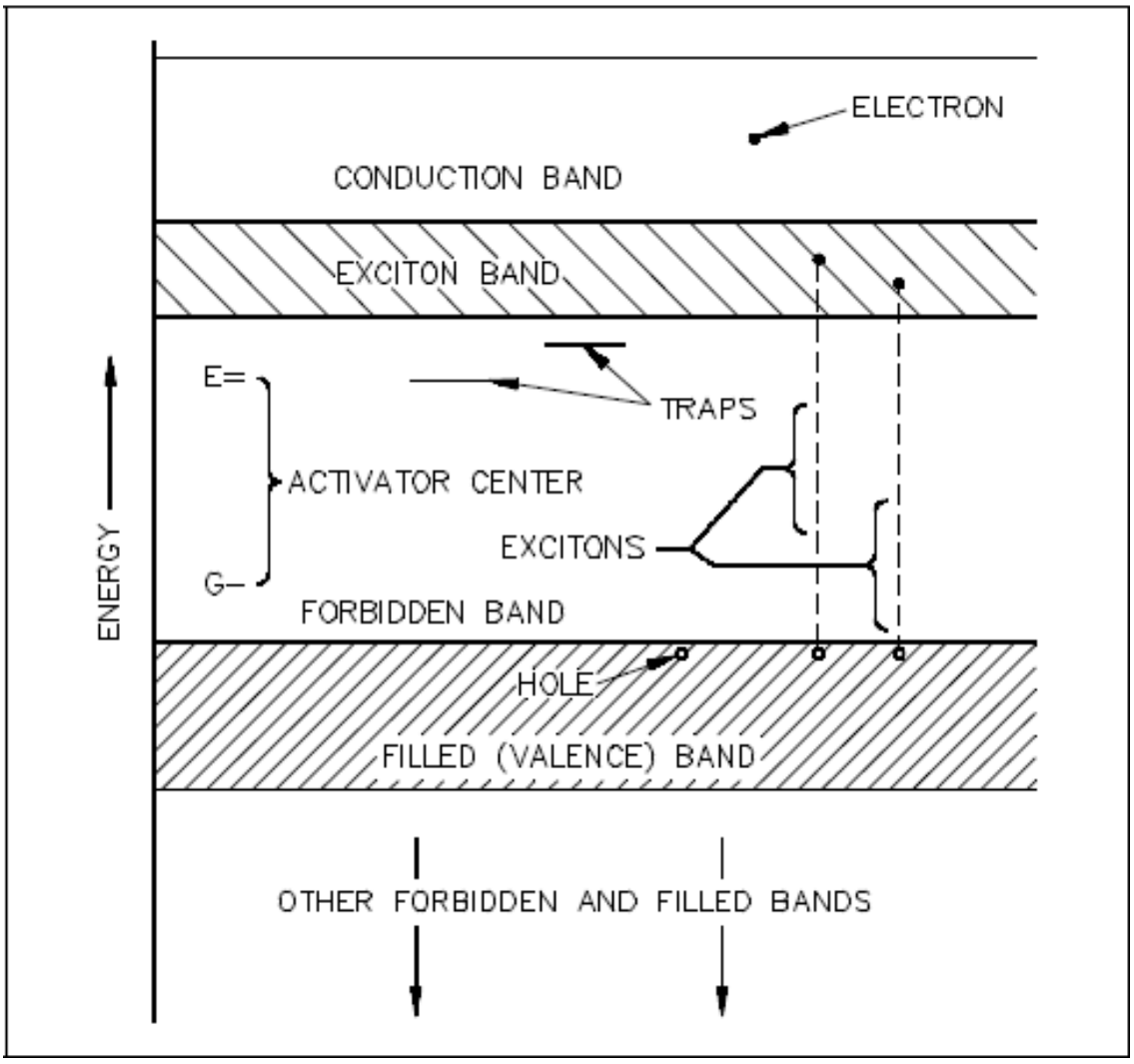

Figure 10: Interactions in the Scintillation Material [8]

Figure 10 shows the result of the interaction of the incident gamma ray with the scintillation material. If the energy transferred to the electron is greater than the ionization energy then the electron jumps to the conduction band otherwise the electron, exists in an excited state. In either case a hole is created in the valence band. If the crystal used is pure, then in the process of de-excitation, a photon is emitted with a very high energy which is not visible to the photomultiplier tube, PMT. If some impurities, known as an activator, are added to

the crystal additional energy levels are added in the forbidden band. The hole that was created in the valence band shifts to the new added energy levels [8] [10]. Thus in the process of de-excitation, a photon is released with an energy equal to the difference between the newly created energy levels and the conduction band. Since the created energy levels are closer to the conduction band, the emitted photon has less energy making it visible to the PMT [8].

The scintillation light is emitted in all directions; hence a reflector is used to minimize the loss of light. Magnesium Oxide, MgO, is commonly used as a reflector [9]. A photo multiplying tube, PMT, is used to convert the emitted light into an electrical signal that can be processed.

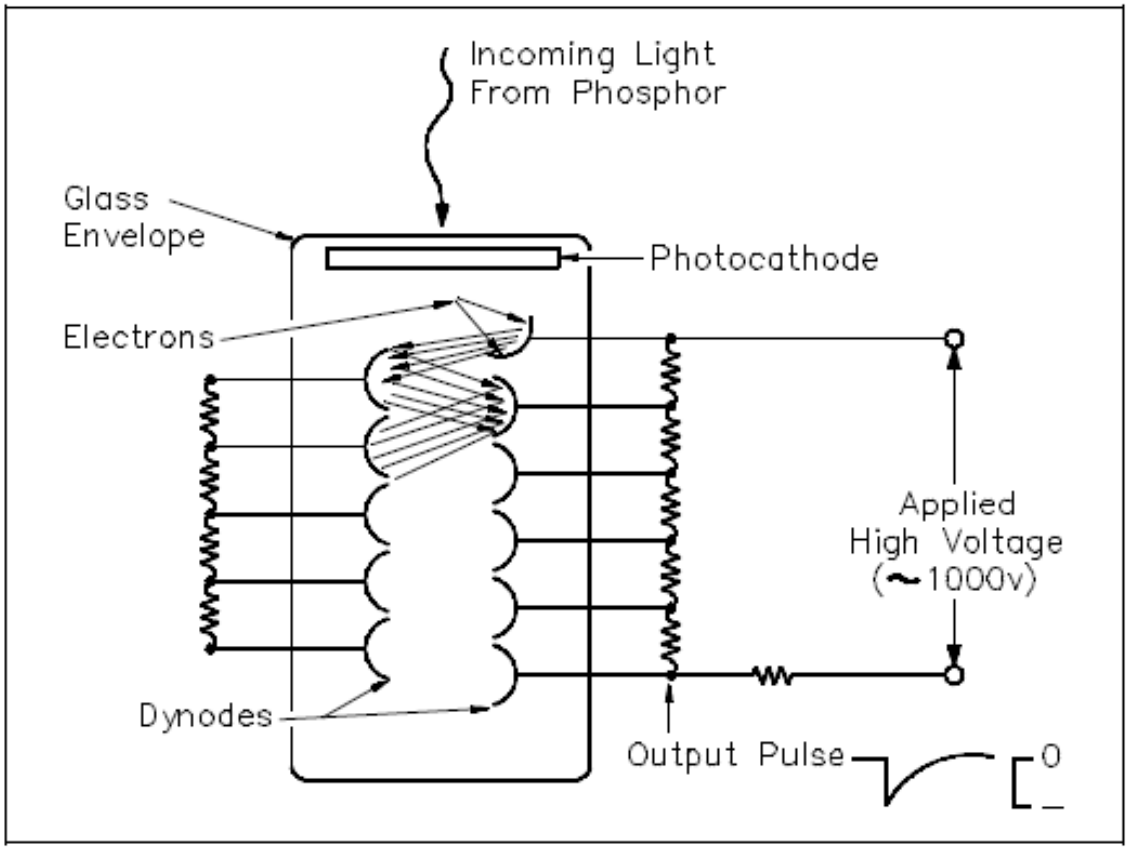

Figure 11: PMT Components [8]

Figure 11 shows the component of a PMT and the operational mechanism. It can be seen that the emitted light is directed to a photocathode where the light will be converted through photoelectric effect into electrons with almost equal energy to the incident light. These ejected electrons are too small in number and energy to be processed by electronics [8]. In the PMT, these electrons are multiplied in energy and numbers through an acceleration process between many dynodes due to a significant voltage drop between each dynode. The amount of electrons generated at the end of this multiplication process is proportional to the amount of energy deposited by the gamma ray. Therefore, scintillation detectors are

used in spectroscopy. The exact number of electrons generated is a function of the applied gain.

2.4.2 Solid-State Detectors

Unlike other types of detectors, solid-state detectors offer great energy resolution for gamma rays. The detection mechanism is similar to that of scintillators, whereby an incident gamma ray will interact with the crystals of the detector causing an electron to be ejected. The ejected electron jumps to the conduction band creating a hole in the valence band. Due to the nature of the semiconducting material used, the electron and the hole created move around freely. Due to the high electric field applied by the bias voltage, the electrons generated move toward the electrodes which then are converted by the preamplifier to a voltage pulse. Both germanium and silicon possess ideal electronic properties that make them perfect candidates for semi-conductor detectors [9].

Materials with a low band gap, which is the case with all semiconductors, tend to have a high probability of thermal excitation leading to the creation of an electron-hole pair [2]. Hence, semi-conducting crystals, such as high purity germanium (HPGe) crystals, must be maintained at a very low temperature around 77 K. Liquid nitrogen is generally used to cool HPGe crystals. Figure 12 illustrates a UOIT high purity germanium (HPGe) detector connected to a nitrogen gas for cooling purposes.

Figure 12: UOIT High Energy Gamma Spectroscopy System

2.4.3 Gas filled Detectors

The family of gas-filled detectors are the most commonly used detectors. They simply consist of a metallic tube filled with a gas. The inner wall of the tube is the cathode and the thin wire in the middle of the detector is the anode [10]. This family of detectors works on the principle that when ionizing radiation interacts inside the detector; along the track of the ionizing particle, electrons and positive ions are created. Depending on the strength of the applied voltage, electrons and positive ions drift to their corresponding electrode. The collection of these charged particles leads to the formation of a pulse across the resistor [2]. This pulse is then registered by the electronic signal processing electronics as a count. Figure 13 illustrates a typical design of a GM detector.

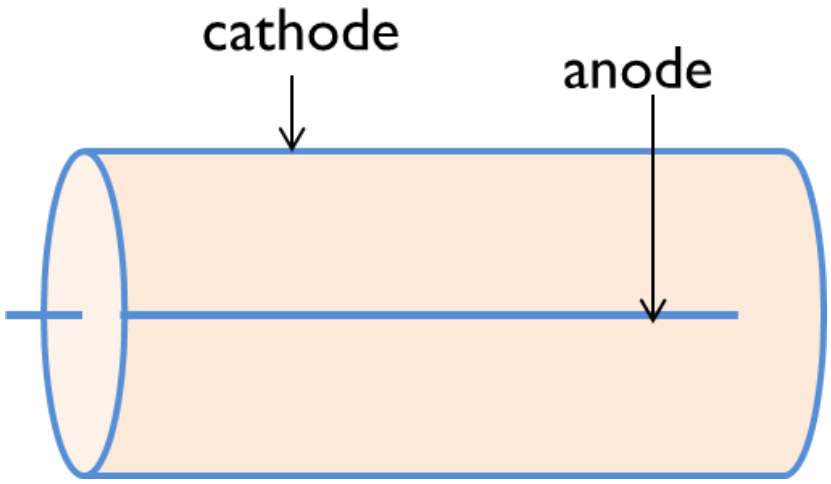

Figure 13: Typical End Window Geiger Muller Detector [2]

As indicated earlier, the variation of the voltage applied between the anode and cathode determines the characteristic of the detector. If the applied voltage is very low, most if not all generated electrons and positive ions recombine. If higher voltage is applied then all generated electrons and positive ions will be collected at the corresponding electrode. The number of electrons collected is the actual number of electrons created and is proportional to the energy deposited by the ionizing particle. This region of detection is known as the *ionization chamber region*. If a higher voltage is applied, then the ejected photoelectrons are accelerated between collisions with the gas atoms and thus inducing further ionization of other gas molecules. The total number of electrons collected is still proportional to the energy of the incident ionization radiation. This region of detection is known as the *proportional counter region*. A further increase in the voltage leads to greater electron multiplication. The number of electrons collected is no longer proportional to the energy of the incident ionizing radiation. This region of detection is known as the *Geiger-Muller*

counter region [10]. Any further increase in voltage will lead to the continuous discharge region. In this region, the voltage is so high to the point where one ionization process will produced a continuous electron multiplication leading to a continuous discharge of the gas [8].

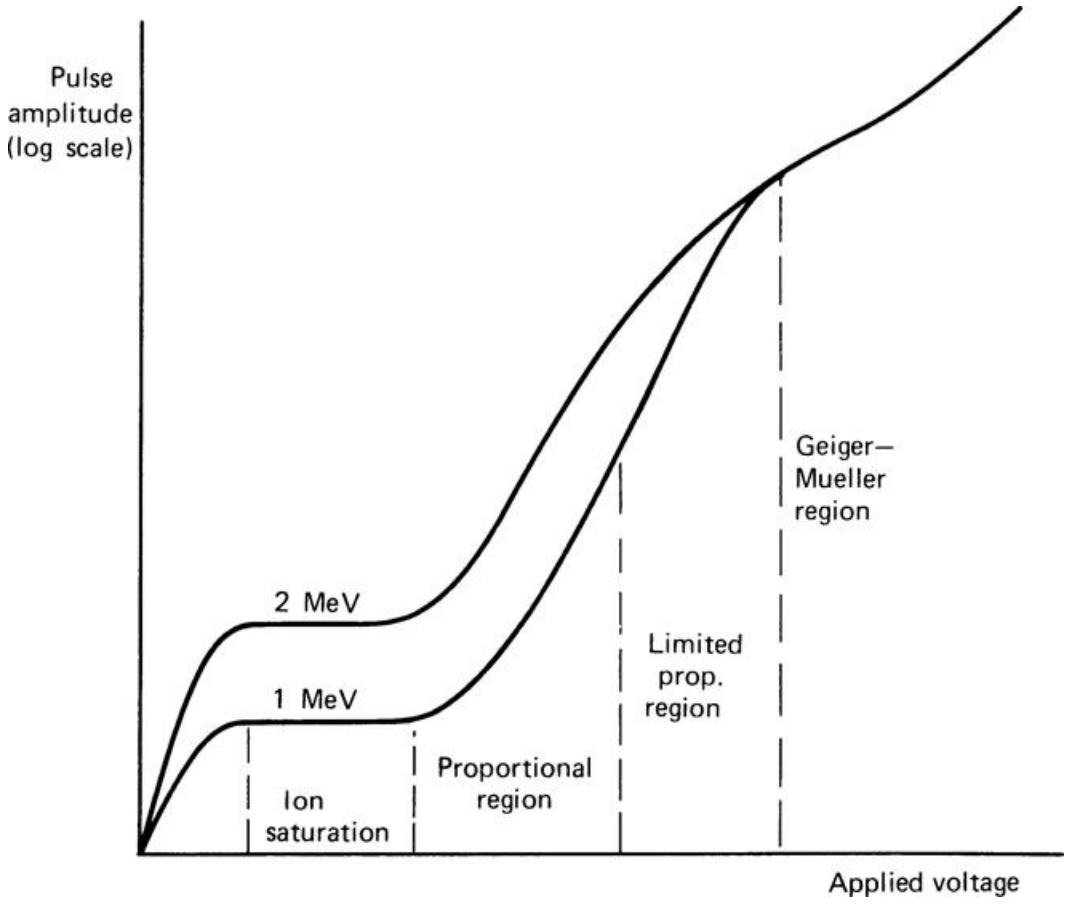

Figure 14: Gas Detector Output vs Applied Voltage [2]

Figure 14 illustrates the various region of detection. Each region of detection has its own application based on its properties. Some detectors, based on their type, may function only as a counter while others are used to determine the intensity and the energy of the incident

particle. A Detector resolution, efficiency and size, and the Z value of the material used, determine the appropriate use of each of these detectors in various scenarios [10].

2.5 Geiger-Muller Detector

The GM detector is one of the oldest detectors. It was developed by Geiger and Muller in 1928. GM detectors are still used worldwide in a variety of applications. The main reason for their continuous survival is attributed to their simplicity and low cost [2]. In this section of the report, a detailed analysis of the detector will be provided. In-depth understanding of the properties and structure of the GM detector will assist in the development of an energy compensated GM detector, which is the main objective of this research.

2.5.1 Townsend Avalanche

As indicated earlier, a GM detector is based on the principle of gas ionization. Incident radiation interacts with either the wall or the gas of a GM detector, leading to ionization of the gas molecules along the track of the charged particle produced. All the electrons and positive ions that are generated will drift toward the appropriate electrode. Gas multiplication takes place due to the high voltage applied within the tube. In this process electrons gain significant kinetic energy from the electric field between collisions. As the electron travels toward the anode it collides with orbital electrons of the neutral gas molecules. In every collision, a significant amount of energy is transferred. If the transferred energy is greater than the ionization energy of the gas molecules, then further ionizations takes place [2]. Each ejected electron is accelerated during a mean free path, due to the high voltage applied, and continues to induce further ionizations. This

multiplication process is known as a *Townsend Avalanche*. Equation 2.11 is used to estimate the total number of electrons produced at any point in the tube [2];

$$n(x) = n_0 e^{\alpha x} \qquad 2.11$$

The α term in Equation 2.11 corresponds to the first Townsend coefficient for the gas which is defined as the number of ion pairs generated per unit length, n_0 represents the initial number of electrons and x is distance travelled. The number of electrons increases in an exponential form as they travel toward the anode.

2.5.2 The Geiger Discharge

The formation of one avalanche can lead to the formation of other avalanches elsewhere in the detector. When an electron collides with orbital electrons along its path, the orbital electron is either ionized or excited, depending on the amount of energy transferred. In the case where excitation takes place, the atom tends to de-excite and, in the process, release a photon. This photon travels in the tube and is eventually absorbed through the photoelectric effect. As a result of the photoelectric effect an electron is ejected. This ejected electron gains some kinetic energy as it drifts toward the anode wire inducing another avalanche [2].

After a set value of electric field, every avalanche can induce another avalanche at a different part of the tube. Within a very short time, many avalanches are formed at different positions along the tube as illustrated in Figure 15. The total number of avalanches formed is always the same regardless of the energy of the incident ionizing radiation. Hence, a GM detector can only function as a counter. In an average size detector, it takes few microseconds for all of the charges to be collected [2].

Electrons are much smaller in size and mass than the positive ions formed hence, electrons travel faster than these positive ions which create a cloud of positive ions which reduce the strength of the electric field in the tube. This reduction in the electric field minimizes the gas multiplication until a point where no further multiplication takes place. This process is known as *Geiger discharge termination*. This termination always takes place when a specific number of positive ions have been formed [2]. Thus the pulse formed due to collected electrons is always of the same size.

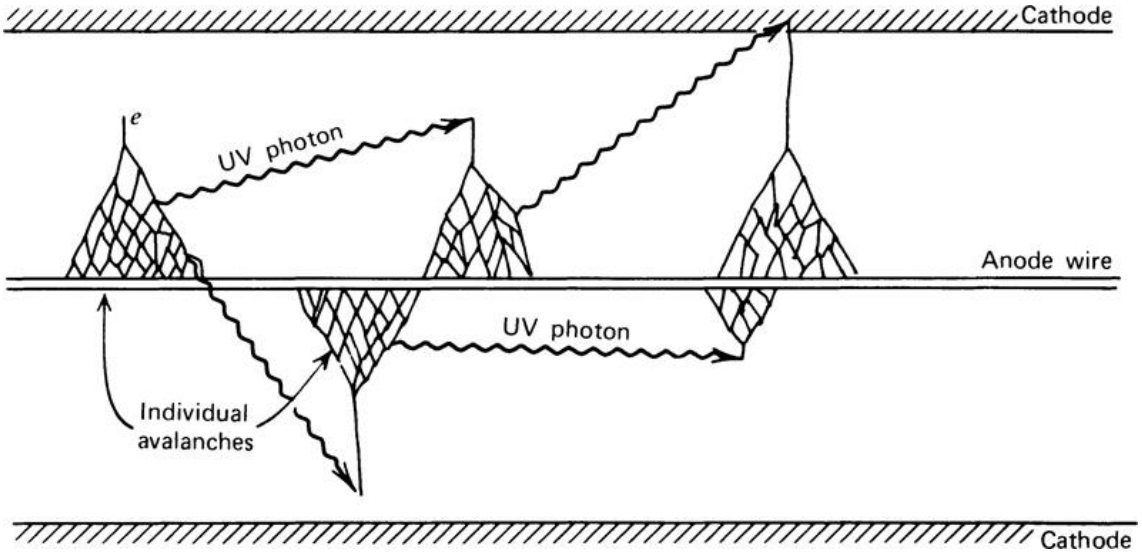

Figure 15: Avalanche Formation [2]

2.5.3 Fill Gas

The most commonly used type of filling gas is an inert gas. Inert gases have a low avalanche multiplication threshold. Below this threshold, secondary ionization will not take place. The density of the gas is a very important factor especially when x or gamma rays are to be detected. The pressure of the gas is usually kept at atmospheric level [2].

2.5.4 Quenching

Due to their size, positive ions generated through ionization tend to move slowly toward the cathode. Once they reach the cathode, they interact with the atoms of the wall's material. As a result, these positive ions combine with the electrons from the wall material and become neutralized. In this process, if sufficient energy is transferred by the positive ion, an electron is liberated. This liberated electron will drift toward the anode and can trigger an avalanche. This process could be repeated many times leading to the formation of multiple pulses. In order to eliminate this problem, two possible methods of quenching may be applied [2].

2.5.4.1 Internal Quenching

In this method of quenching, a quenching gas is added to the gas mixture. The role of quenching is to eliminate the liberation of electrons from cathode due to the interaction with positive ions. This is accomplished through neutralizing the positive ions of primary gas by the quenching gas. The positive ions of the quenching gas drift toward the cathode and interact with it in an attempt to be neutralized. If the positive ions of the quenching gas have excess energy, then this energy will not be used to liberate an electron from the cathode but will be used to disassociate the complex molecules [8] [2].

The quenching gas is carefully selected to have a lower ionization potential so it is easily ionized as with the primary gas mix. The quenching gas should also have a more complex molecular structure. The typical percentage of quenching gas is around 5 to 10 %. The most commonly used type of quenching gas are halogens such as bromine or chlorine [2].

2.5.4.2 External Quenching

External quenching is the second method used to eliminate the production of secondary pulses due to the liberation of electrons in the process of neutralizing positive ions. The liberated electron through the neutralizing process is only able to create an avalanche if the potential difference between the cathode and the anode is higher than the minimum required potential differences [2]. Therefore after the formation of each pulse, the applied voltage is reduced for a fixed time to ensure that any liberated electron during this time is not causing an avalanche. The internal quenching method seems to be more commonly used than the external quenching method.

2.5.5 Pulse Formation

A GM detector functions in a pulse operation mode. This mode of operation is able to provide information related to the amplitude i.e. the number of collected charges as well as the timing of each pulse event. Other modes of operation, such as the current mode and the mean square voltage mode are unable to provide this information [2].

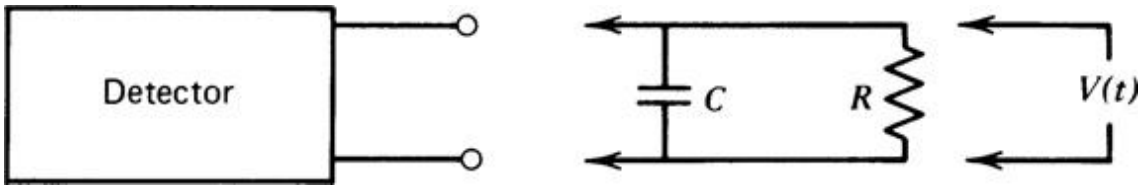

Figure 16: GM Detector Circuit [2]

The shape of the pulse formed is directly related to the characteristics of the circuit to which the detector is connected. The sketch in Figure 16 represents the general circuit connected to a GM detector. The R in the sketch represents the resistance of the circuit, whereas the C represents the capacitance of the detector and the measuring circuit, and V (t) in the sketch represents the time-dependent voltage applied across the resistance. The electrons collected at the anode flow into the capacitor. The time period associated with the collection of all electrons is known as the *collection time*. After all the electrons have been collected at the capacitance, the capacitor discharges all collected electrons through the resistor. As a result, the voltage across the load resistance is restored to zero. The size of each pulse is a reflection of the amount of charge collected at the anode. In the case of the GM detector, the total number of electrons collected is always the same hence all the pulses formed have the same height. The number of pulses formed is a reflection of the rate of radiation interaction within the detector [2].

2.5.6 Dead Time and Recovery Time

Due to their size, electrons are collected much faster at the anode wire and get processed. On the other hand, positive ions formed are much larger in size hence they drift very slowly to the cathode. The collection of electrons gives rise to a pulse at the output of the electronics circuit. The process requires a minimum time during which the detector is unable to detect any other particles. The detector during this time is considered dead. The technical definition of a dead time is the time difference between a pulse and the time at which a second Geiger discharge can occur regardless of its size. Figure 17 illustrates the dead time and the recovery time of a GM counter [2].

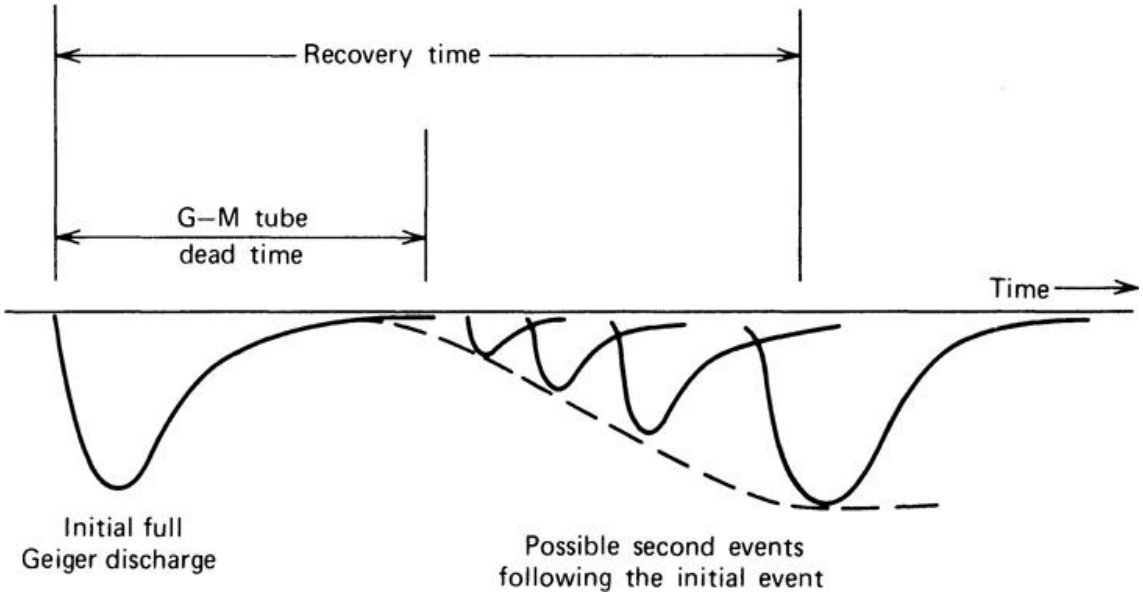

Figure 17: GM Detector Dead/ Recovery Time [2]

The dead time varies depending on the size of the detector and the filling gas as well as the gas pressure inside the detector. The average dead time of an average GM detector is in the range of 50 to 100μs. After the dead time elapses the detector is able to generate a Geiger discharge however, the initial discharges after the dead time has elapsed are not a full discharge [2]. A full discharge only occurs when the detector is in the initial operating conditions. The time difference between one full discharge and the second full discharge is known as the recovery time.

2.5.7 Geiger Muller Response to Gamma rays

A single ionization event inside the gas is sufficient to induce a Geiger discharge in a GM detector. Therefore the efficiency of the GM detector generally depends on the incident radiation and its ability to induce ionization inside the gas. Gamma rays have a very high penetrating power hence it has a very low detection efficiency. Detection of Beta and alpha

particle is a result of the direct interaction of these particles with the gas atoms in the detector. Gamma ray detection on the other hand is mainly a result of the interaction of the gamma particle with the cathode wall. The gamma ray interacts with the detector wall's atoms through one of the three common methods of interactions. An electron is ejected as a result of the interaction. If the ejected electron is able to enter the gas volume of the detector before the end of its track then the gamma will be detected. As mentioned earlier the probability of gamma interaction is generally governed by the Z value of the material of interaction and the energy of the incident gamma. The higher the Z value, the higher the probability of interaction. Stainless steel which consists mainly of chromium iron is widely used as a cathode material for GM detectors. Bismuth and lead are also used as a material for the cathode wall. Also if the interaction of the incident gamma takes place further inside the wall, then the probability of the ejected electron to enter the gas volume is higher as illustrated in Figure 18. Therefore the thickness of the wall of the detector is a crucial factor for the detection of gamma rays. The common thickness used is 2 mm.

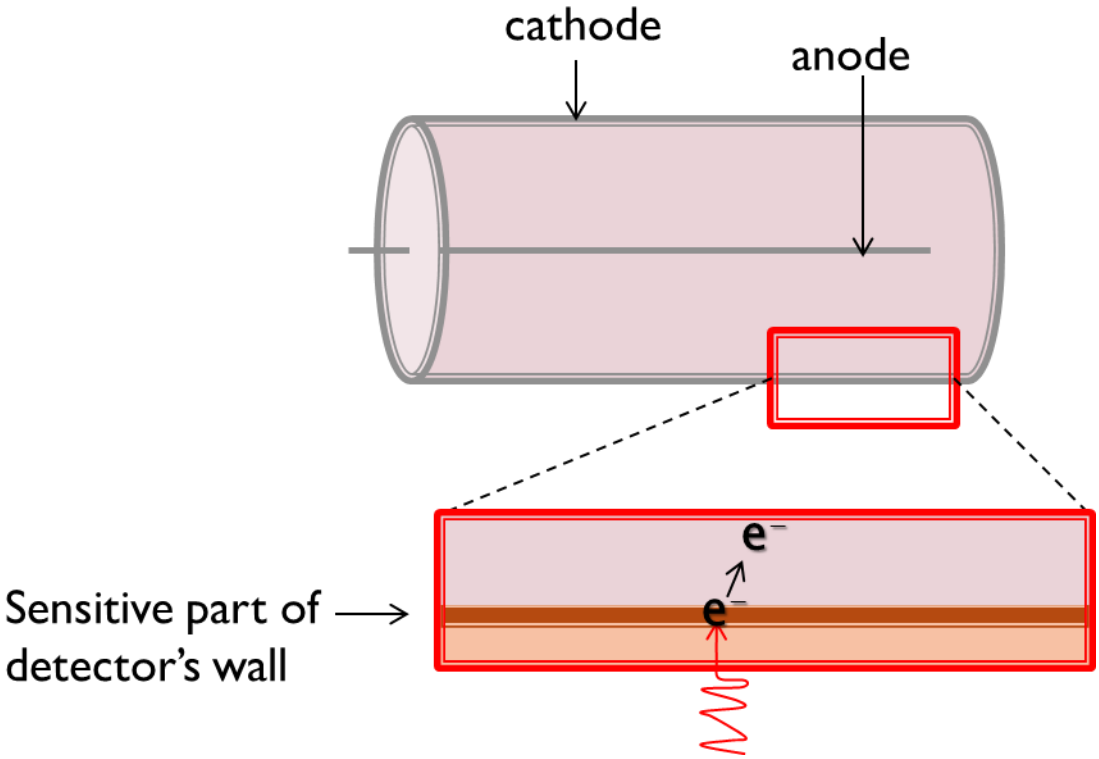

Figure 18: Gamma ray Attenuating GM Detector Wall

A GM detector response to gamma rays varies with the energy of the incident gamma ray. Gamma rays with energies less than 120 keV have a higher response than gamma rays with higher energies. The over response is mainly due to the variation of cross-section with gamma energy. The cross-section is basically the probability of interaction of the incident particle with target atoms and it has the unit of per cm^2. Higher cross-section is simply higher probability of interaction hence higher counts. Figure 19 shows the attenuation cross-section of iron as a function of gamma energy. Most if not all elements have the same trend when it comes to the cross-section as a function of gamma energies.

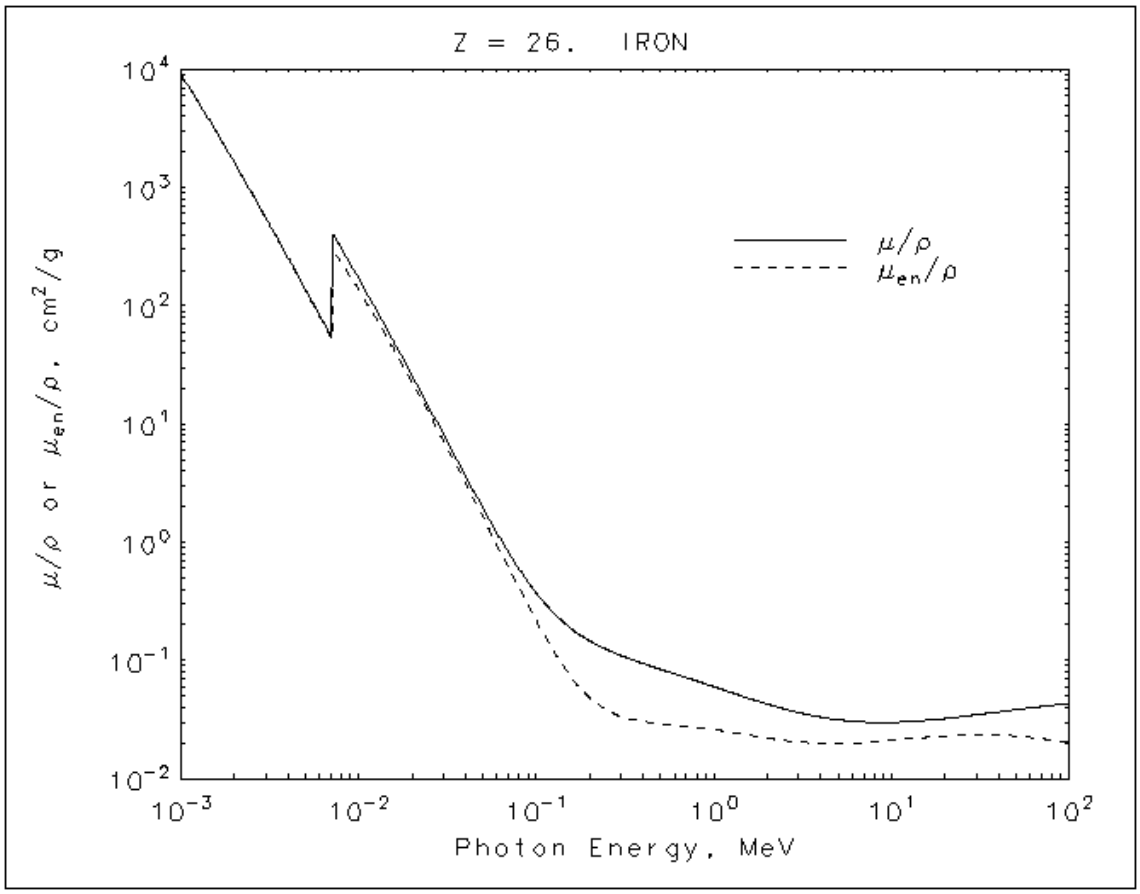

Figure 19: Iron Mass Attenuation Coefficient

Figure 19 shows the mass attenuation coefficient for iron which is the main component of the cathode wall of the T2416A. For instance, the mass attenuation coefficient for photons with energy of 20 keV is 1000 times higher than the mass attenuation coefficient for gamma rays with energy of 200 keV. This great difference in the cross-section is the main reason for the over response of the GM detector. Further analysis of Figure 19 leads to the observation of a sudden decrease in the cross-section from high to low energy photons which is known as the *absorption edge*. As the gamma ray energy decreases beyond the binding energy of the K, L or M shell electrons, the probability of interaction with electrons in this shell comes to an end thus the sudden decrease in the cross section. The utilization

of this phenomenon is a key factor to the optimisation of the response function of the GM detector. Next chapter contains a detail description of the methodology for optimizing the response of the GM detector.

Chapter 3: **Methodology Description**

3.1. Response Function of GM Detector

Before discussing the methodology applied to achieve an improved response from the T2416A GM detector, the nature of the over response of the detectors will be discussed in this chapter. To illustrate the problem, Figure 20 shows the general trend of the response of a GM detector to gamma rays with low energies.

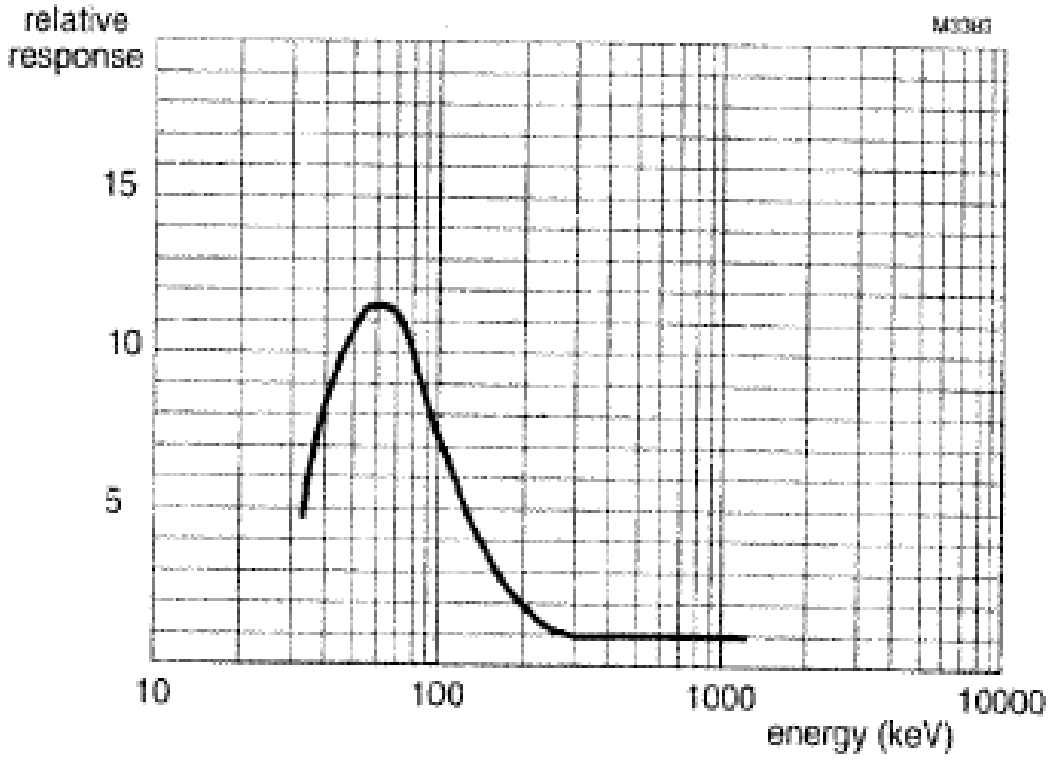

Figure 20: General Trend of GM Detector Response Function (courtesy Centronic)

From the graph, it can be concluded that the area of over response is between 30 and 200 keV. An over response here is referred to the measured response at a specific energy divided by the response of the detector at a reference energy (i.e. dose rate measured/dose rate calculated at a fixed distance). For instance, at 30 keV, the GM detector demonstrates an over response by a factor of five and reaches maximum over response by a factor of 12 at around 60 keV. The response function of the GM detector smoothly decreases until it reaches a constant level of response for energies higher than 250 keV. The transfer of a regular GM detector to an energy compensated GM detector requires lowering the over response to gamma rays with low energies. This requires an understanding of the physical parameters involved in this over response, as well the gamma rays detection mechanism.

As previously indicated, the thickness of the GM detector wall plays a very important role in the response function of the counter. An incident gamma ray interacts with the atoms of the wall via one of the three common modes of interactions. As a result of either of these modes of interactions, a photoelectron is ejected. The detector is able to sense the incident gamma if the ejected photoelectron is able to enter the sensitive volume of the detector, i.e. the gas region. The probability of the ejected photoelectron entering the gas region depends on the energy of the incident gamma ray, and partially on the material of which the wall of the detector is composed. The incident gamma ray must have enough energy to almost penetrate the detector wall and interact further inside the wall so that the ejected photoelectron has enough energy to enter the gas volume before the end of its range. An area in the inner side of the wall is recognized as the sensitive part of the wall. Any interaction of an incident gamma ray outside of this area will not be counted by the detector. The thickness of this area is determined by the range of the ejected photoelectron with the

maximum possible energy. The maximum energy can be transferred to the photoelectron when the mode of interaction is the photoelectric effect with the highest possible energy. Details of the photoelectric effect interaction were described in chapter 2.

The photoelectric effect for the most commonly used materials for a GM detector wall is dominant for gamma rays up to energies around 200 keV. Therefore, the maximum energy that can be transferred to a photoelectron is when the incident gamma ray has energy around 200 keV and the mode of interaction is the photoelectric effect. The energy transferred to the photoelectron can be calculated according to equation 2.2.

The binding energy of the K electron for iron, the main component of the detector wall, is around 7.12 keV. Hence the ejected electron has an energy that is approximately equal to 192.88 keV. Using Figure 21, the range of such an electron was determined to be around 0.5 μm. The wall thickness of the T2416A detector is around 80 μm. Therefore only gamma rays with sufficient energies are able to penetrate to the sensitive part of the wall where a photoelectric effect may take place and produce a photoelectron. This photoelectron is able to enter the gas region and produce a count. Increasing the size of the wall attenuates gamma rays with low energy, hence lowering their probability of reaching the sensitive part of the detector wall and producing a count.

The main reason for the over response of the counter is the high probability of interaction of gamma rays with low energies (cross section of the gamma interaction with a specific material). Thus, increasing the thickness of the wall tends to lower the probability of low energy gamma ray to reach the sensitive part of the detector wall and consequently reduces the counter over response.

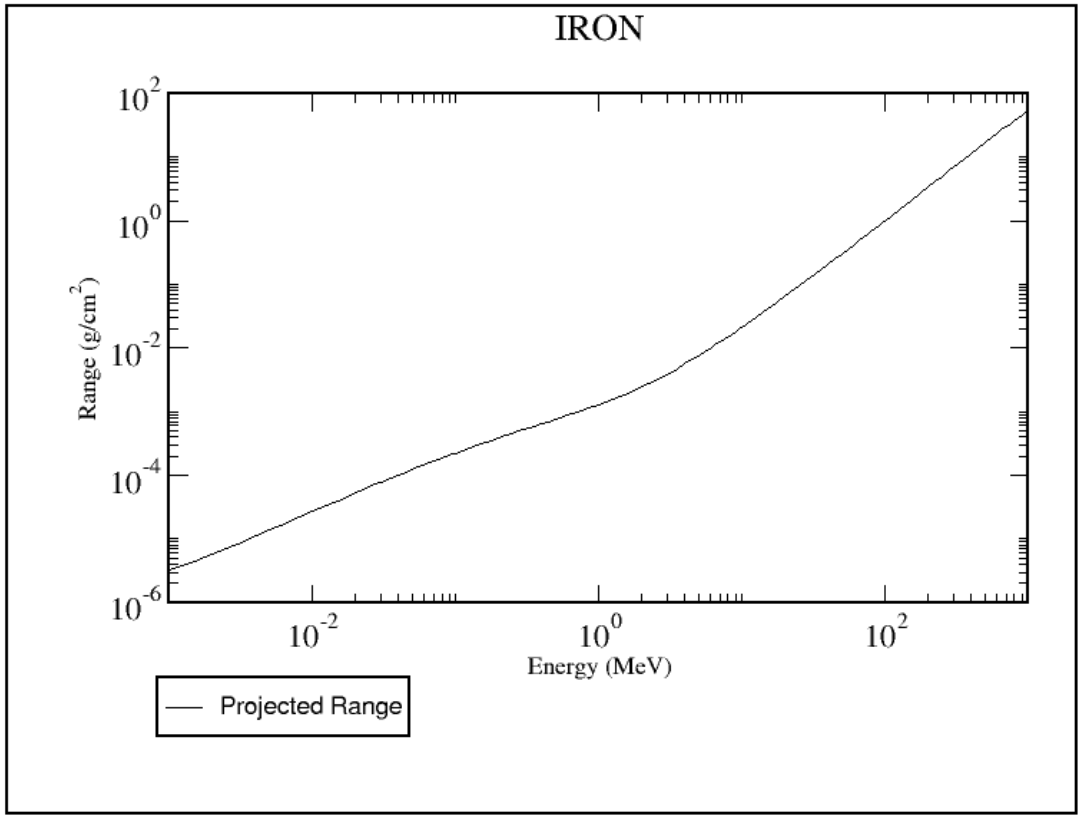

Figure 21: Projected Range of Electrons in Iron [11]

However, instead of increasing the thickness of the detector wall, it would be more efficient to cover the detector with another material that has a higher cross-section for gamma rays with low energies and minimum influence on high energy gamma ray interaction. By doing so, the probability of the incident gamma ray with low energy to reach the sensitive part of the detector will be further decreased. This probability can be even further decreased if the chosen material has an absorption edge within the desired range of energies. The cross-section of all elements smoothly increases from high to low gamma energies. This increase is interrupted by sudden decrease of the cross-section, which is known as the absorption *edge.* (The explanation of the absorption edge was discussed in section 2.5.7.) The degree

of decrease due to an absorption edge varies according to the element and the type of edge itself; i.e. K, L, M…etc. The energy at which the K, L or M absorption takes place varies from one element to another. The K absorption edge leads to the highest amount of decrease in the cross-section. For instance, the decrease in the lead cross-section, due to the K absorption edge, at 88 keV is a factor of 10. Thus, the material(s) selected for the filtering purpose should have a K absorption edge in the range of 30 to 200 keV. Wrapping the detector with such a material(s) will lower the response of the detector for gamma rays with low energies. The thickness of the filtering material used was calculated using equation 2.10.

Knowing the ratio, by which the response of the GM detector should be lowered, determines the appropriate thickness to be used. In this case, for 56 keV the ratio is a factor of 20 comparing to 220 keV. The appropriate thickness would depend on the components of the filtering material being used. In addition, the task of lowering the response function of the T2416A GM detector can be achieved by applying the appropriate design features. As part of this work, two main design features have been investigated. In the following sections, details associated with each investigation are discussed.

3.2 Using a Different Wrapping Mechanism

There are many creative ways of wrapping the T2416A GM detector with the appropriate filtering material. In this investigation, and to simplify the design from a manufacturing perspective, only two methods have been considered. A brief explanation of each wrapping method is provided in the following sections.

3.2.1 Using a One-Piece Wrapping Model

A piece of filtering material made from tin has been used to cover the entire detector. Due to the large cross-section in lower energy, it is expected to significantly lower the response of the T2416A. The response function of the T2416A with this method has been simulated in MCNP/X.

3.2.2 Using a Two-Piece Wrapping Model

In the second method, two pieces of a filtering material have been used to partially cover the detector wall. Tin filtering material has been used to construct both pieces of the filter. The impact of this method on the response of the T2416A GM detectors has also been simulated in MCNP/X. Figure 22 shows the second method for wrapping the detector. An assumption was made, based on an ideal response function; i.e. the gap width has been chosen in order to minimize the over response.

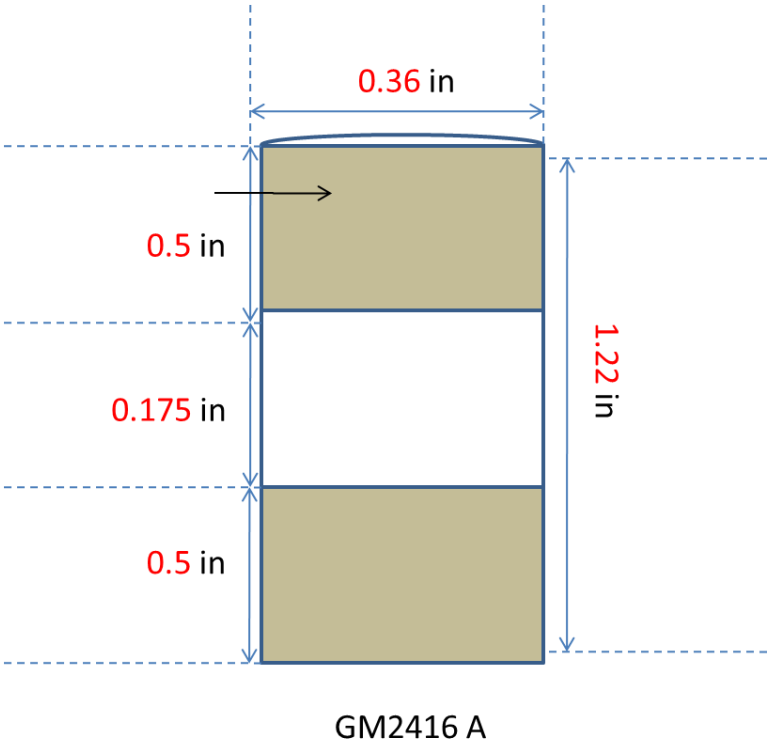

Figure 22: Two-Piece Wrapping Model

3.3 Using an Appropriate Filtering Material

As discussed in the previous section, a potential filtering material should have:

- A cross section higher than the material of the detector wall; i.e. Fe.
- An absorption edge that falls within the range of 30 to 200 keV

Few elements fit the set criteria, such as: tungsten, gold, platinum, tin and lead. The latter two materials are the most commonly used for the purpose of gamma ray attenuation due to their well-known properties, availability and low cost.

3.3.1 Using Single Filtering Material

As part of determining the appropriate filtering material to lower the response of the counter in specific regions of energy, two materials have been investigated: namely, lead and tin. The impact of each in lowering the over response of the T2416A GM detector was determined. For lead, both experiments and simulations have been performed. However, only simulations were performed for tin.

3.3.2. Using a Combination of Materials

To lower the over response of the T2416A GM detector over a wider range of gamma ray energies, a filtering material composed of various combinations of both lead and tin was also investigated. The impact of these design features was investigated through the use of an MCNP/X simulation model built to determine the response function of the T2416A GM detector.

As will be seen in chapter 4, different materials such as lead and tin do not significantly differ in their cross-section in the energy range of 50-250 keV. However, in the range of low energies, i.e. 20 to 50 keV, the difference in the cross-section is remarkable. Thus two sets of simulations were performed. The first set was developed to validate the performed experiment conducted in the energy range of 50 to 250 keV. The calculated number of counts from the simulation per source particle was normalized to the measured intensity of the source. The dose rate was then calculated after extraction of the fluence at a specific distance. Equation 3.1 was used to determine the dose-equivalent rate which is defined as the absorbed does per unit time.

$$\dot{H} = \Phi \times cf \qquad 3.5.1$$

$\dot{H}$ is the ambient dose-equivalent rate in Sv/hr, Φ is the flux in $\frac{\#\ of\ Particles}{cm^2.Sec}$ and cf is the conversion factor in pSv.cm^2. All obtained results are presented and discussed in chapter 4, where the dose equivalent rate is plotted as a function of gamma ray energy. The second set of simulations was performed to examine the response function of the counter for energies lower than 50 keV. In this part, the GM, with and without filtering material, has been exposed to low energy gamma rays at a fixed distance, and the number of counts has been obtained. However, due to lack of intensity of the source in this region, the dose rate was not calculated. Instead, the number of counts per source particle was determined and plotted as a function of gamma ray energy. It should be noted that the results obtained in this region are for quality analysis, in order to provide insight into the impact of different filtering materials, both homogenous and heterogeneous, and different thicknesses. Results from these simulations are presented in Appendix E.

3.4 MCNP/X Simulation

Monte Carlo N-Particle (MCNP) is a modelling code that was developed by Los Alamos National Laboratory during the Manhattan project in the 1940s. It is considered as one of the most powerful modelling codes for particle transport. The MCNP modelling is based on tracking particle(s) from its birth to its death. The latest version of MCNPX is capable of tracking 34 different particles such as alpha, beta, gamma, neutron, and positron. It is also capable of tracking a combination of particles with a very wide range of energies. For instance, photons with energies between 1 keV and 100 GeV can be tracked using MCNPX.

MCNP has been used in many applications such as reactor designs, radiation detection, nuclear medicine, as well as for military applications. Due to the various possible applications of MCNP, the US government has very strict regulations for accessing the code.

3.4.1 MCNP Input File

In order for MCNP to model any scenario, the user must provide the details of the scenario. The user must also provide what type of calculations or output MCNP should provide. There are three essential sections of the input file. Each section deals with specific information related to the scenario problem being modeled. The details of each of these three sections are provided below.

1. Cell Card

In this section of the input file, the various regions and volumes in the scenario are defined along with their materials. Cells are determined by intersections, unions and complements of surfaces. Each cell is defined by four parameters. The first parameter is the cell number. This number is selected by the user to define a specific cell. The second parameter is the reference number of the material used to fill this cell. In the case where the cell is void, a value of zero is given. The density is the third parameter of the cell card. A negative sign always precedes this value for a mass density of $\frac{g}{cm^3}$. If the cell is void, then this parameter remains blank. The fourth parameter defines the boundaries of the cell through union or intersection operations of the defined surfaces.

2. Surface Card

In this section of the input file, the user defines the reference position of the geometrical shape in the three-dimensional space. There is a list of predefined surfaces that are used to create the desired geometry. A used selected number is used to define the surface. One of the predefined shapes is then used to determine the geometry of the shape. For instance, a cylinder is defined by the letter C. If the cylinder is on one of the x-axis, then the letter representing that axis will follow the letter C. However, if the cylinder is parallel to the axes (x, y, z), then the letter C is followed by a forward slash and the letter representing the axis to which the cylinder is parallel. The x, y and z coordinates, through which the cylinder's axis pass, are then defined. The coordinate of the axis, to which the cylinder is parallel, does not have to be indicated. The radius of the cylinder is then defined by the user following the two coordinates. For example, 1 C/Z 4 4 4 represents surface number one, which is a cylinder that is parallel to the z-axis, and the axis of the cylinder passes through the points 4,4,0 and has a radius of 4. The MCNP/X manual contains a table of all the available shapes that can be used, along with their respective representations.

3. Data Card

This section of the input file contains information specifying the material cross-section, source and tally information. The material specification card lists the isotopes used in each material along with the cross-section for all cells containing such a material. Each material has a reference number selected by the user.

The type of particles to be tracked has to be defined by the user in the mode card. The default mode is neutron tracking. As indicated earlier, a combination of tracking, such as n, p or n, p, e., can be used.

MCNP/X allows the use of different types and shapes of radiation sources. The user has to define the desired source and the desired shape of the source. The user may also define the energy of the source, the position and the distribution of the source. The user has then to determine the desired output of the simulation. There are various predefined tallies, such as currents across a surface, a flux at a point and the track length estimates of cell flux. A total of 22 tallies can be used in MCNP/X. A user may use more than one tally. The tally output is always normalized to be per source particle. The output is verified by MCNP/X code to ensure the output passes a series of statistical verifications.

3.4.2 Geometry Model of GM detector

Table 1 lists the characteristics of the T2416A GM detector. These characteristics were used to build the MCNPX model that simulates the response function of the T2416A GM detector.

Table 1: T2416A Spicifications

Characteristics	**Values**
Sensitivity (Cs-137 cpm at 1mR/h)	420
Recommended voltage	575
Plateau length	500-650
Plateau Slope (%100 V max.)	8
Dead time (μs)	45
Background (cpm)	12 max
Resistor Ra ($M\Omega$)	4.7
Cathode material	Cr/Fe
Cathode wall	64-80 mg/cm^2
Max. Overall length (mm, in.)	5.1, 2.0
Max. Overall Diameter (mm, in.)	10, 0.4

3.4.3 MCNP/ MCNPX Visual Editor

The visual editor is a component of MCNP that was developed to assist the user in creating the input file. The visual editor was introduced in the 5th version of MCNP in 1997. Through the visual editor, the user is able to modify and establish many parameters of the input file in a user friendly medium. The user is also able to view a three-dimensional view of the modeled geometry. Figure 23 shows a three-dimensional view of one of the models of T2416A GM detector used in the simulation with the two pieces filtering material wrapping method. The input file shown in Figure 23 is provided in Appendix A.

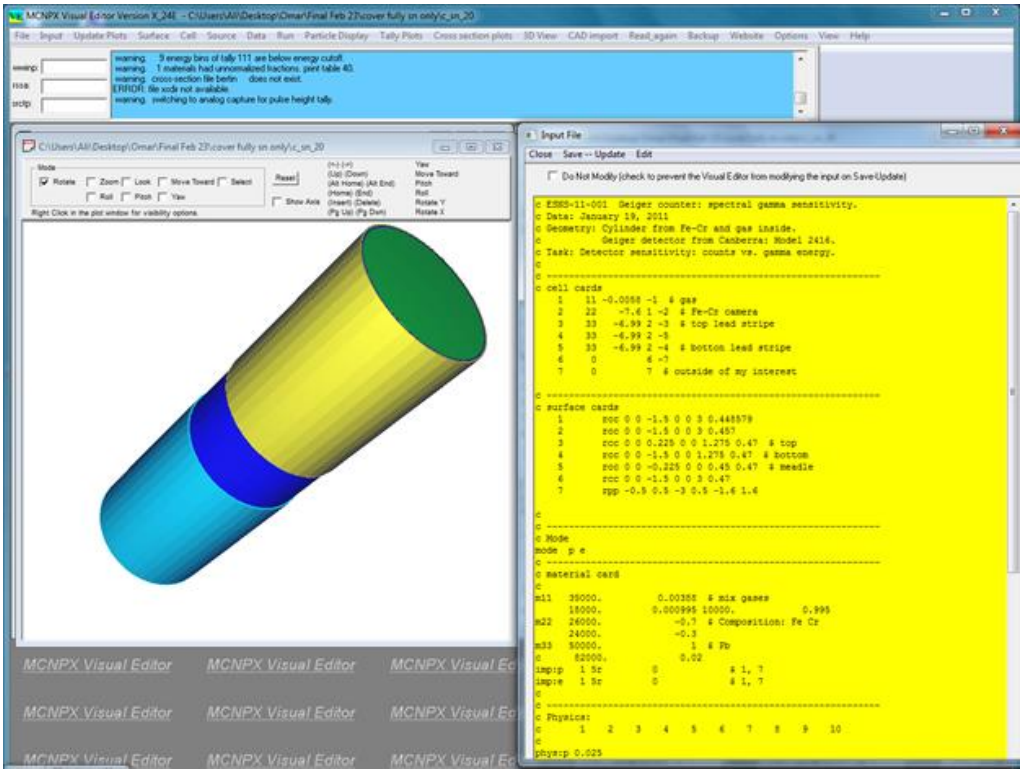

Figure 23: MCNPX Visual Editor

3.5 Experimental Investigation

A series of experimental investigations were carried out to validate the results obtained in the performed calculations with MCNP/X. The experiments were conducted at the Canberra Co. site of the Dover facility, NJ, USA. The purpose of these experiments was to determine the response of the GM detector, with and without shielding material, to gamma rays with various energies. Knowing the exact over response of the detector from the experimental measurements provides a quantitative tool to approach the optimization process.

3.5.1 Experimental Setup description

In this section, a detailed description of the experimental procedure is given. Eight T2416A GM detectors were used; i.e. four detectors covered with filtering materials, and four which were not. A total of 14 experiments were conducted:

1. Before being shipped to the Dover facility for experiment, all detectors passed the QA inspection (see Figure 25) in terms of operating voltage for an optimum range of their plateau, at the Canberra site in Concord.
2. The appropriate filter was placed on the X-ray machine to provide the desired energies, starting from 56 to 222 keV provided by a standard X-ray machine.
3. A certified detector (Centronic energy compensated GM counter) was used to determine the appropriate distance for a constant dose rate (see Table 2). The values of the dose rate measured with such a GM tube were within 20% accuracy.
4. Each of the eight used detectors, operated under an optimum of 575 V, was placed at the determined distance and exposed to various X-ray energies as shown in Table 2 and as illustrated in Figure 24 and the dose rate corresponding to the measured counts was determined using equation 3.5.2.

$$D_2 = \frac{D_1 \times CR1}{CR2} \qquad 3.5.2$$

Where: CR1 and CR2 correspond to the count rate measured by the Centronic counter and T2416A, respectively.

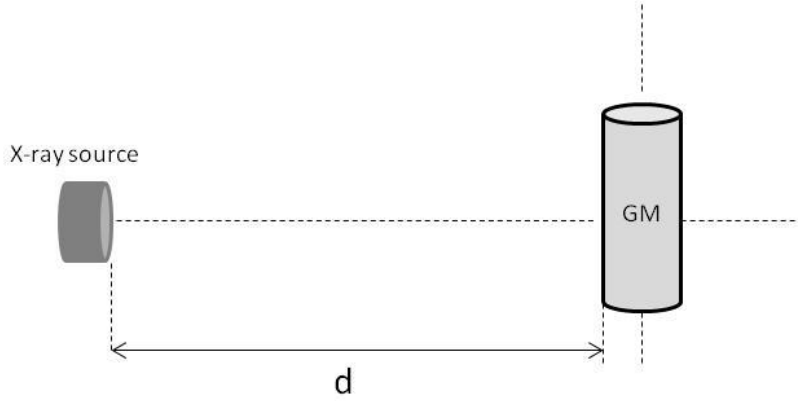

Figure 24: Experimental Setup

Table 2: Parameters of the experimental setup

Energy KeV	Distance cm	Conversion Factor pSv. cm^2
56	64	508
85	145	549
129	130	787
178	95	1079
222	52	1317

Figure 25: Concord QA Inspection Facility

3.5.2 Data Processing

Data obtained from both simulations and experiments were processed using Origin-Pro 9.0 software in different steps:

- The dose rate has been measured with well calibrated equipment as mentioned in section 3.5.1
- The flux of the incident photons has been extracted from the value of the measured dose rate using Equation 3.5.1.
- Using the photon flux determined for each energy and distance, the total number of photons emitted per unit of time (emission rate in 4π) from the source was then calculated.
- The count rate per photon obtained from the MCNP simulation was then multiplied by the calculated emission rate, in the previous step, in order to obtain the total number of counts per second (normalization).

- The flux for a specific energy (at a specific distance, r) was then calculated by dividing the total number of counts per second by $4\pi r^2$
- The dose rate per cm^2 was calculated by multiplying the obtained flux in the previous step by the appropriate fluence to dose conversion factor.
- Finally the total dose rate was obtained by multiplying the dose rate per cm^2 by the area of the detector facing the source.

Regarding the uncertainty, only statistical error has been considered as a square root of the measured counts and no systematical error was included.

Chapter 4: **Results and Discussion**

A total of fourteen experiments were conducted, in addition to the extensive calculations to simulate the response function of the T2416A GM detector, using a wide range of low energy gamma rays and various modifications to the simulation, with various design features. The T2416A GM detector was either with or without a filtering material. The main design features investigated were: the use of different wrapping mechanisms and the use of an appropriate filtering material. In this chapter, the results are presented, analyzed and discussed. The simulation data are presented first, and then compared to the experimental work.

4.1. Response Function of the T2416A GM Detector

In the following sections, results obtained from both experimental work and simulations are presented and the impact of each of the selected design features is discussed. Results are presented in the following order:

- Response function of a bare T2416A GM detector
- Response function of T2416A using two different wrapping mechanisms
    - One-Piece wrapping model that covers the lateral surface of the detector
    - Two-Piece wrapping model that partially covers the lateral surface of the detector
- Response function of the T2416A GM detector using a single filtering material with different thicknesses:

- Lead filtering material
- Tin filtering material

- Response function of T2416A using a combination of filtering material with different thicknesses:
  - 30% Pb and 70% Sn
  - 2% Pb and 98% Sn

4.1.1 Simulation results For the Bare T2416A GM Detector

In the MCNP/X code, a T2416A GM detector was modelled as per the specifications listed in Table 1. To simulate the response function of the T2416A detector to gamma rays with low energies, the T2416A detector was exposed to the same gamma ray energies used in the experiments, namely 56, 85, 129, 178 and 222 keV.

The relative response of the T2416A GM detector to these fields of gamma rays has been plotted using the obtained dose-equivalent rate against the incident photon energy. Figure 26 represents the response function in terms of dose rate of the T2416A GM detector without any filtering material, i.e. a bare detector.

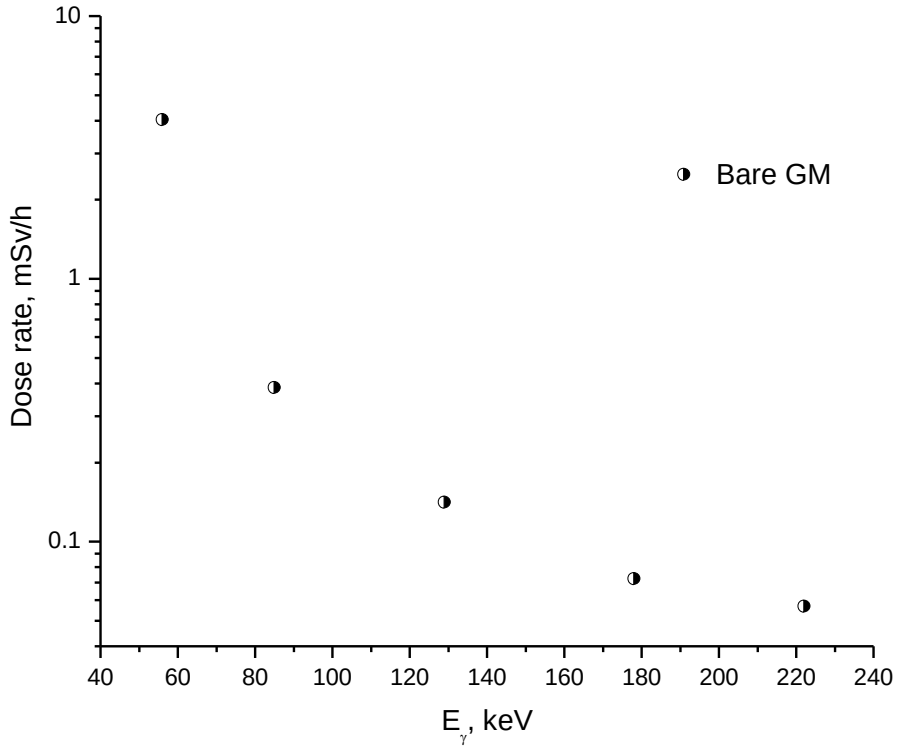

Figure 26: Response Function of T2416A GM Detector Based on the Simulation Data

As expected, the T2416A GM detector demonstrated an over response to gamma rays with low energies; i.e. lower than 200 keV. At 56 keV, the over response is by a factor of 80 compared to 222 keV. At this energy, most of the gamma rays are able to penetrate deeply inside the detector wall and interact via a photoelectric effect. The majority of the ejected photoelectrons are able to reach the sensitive part of the detector, i.e. the gas region.

As the gamma ray energy increases beyond 56 keV, the probability of the dominant mode of interaction (photoelectric effect) drastically decreases since it is inversely proportional to the incident gamma ray energy to the power of 3.5 as per equation 2.3. As the probability of the photoelectric effect interaction decreases, the probability of Compton scattering

increases and dominates for gamma rays with energies greater than 0.5 MeV. The probability of gamma rays interacting through Compton scattering is governed by Equation 2.7.

Unlike the photoelectric effect, Compton scattering has less dependency on both the Z value and the energy of the gamma ray. Hence, the cross section flattens at energies higher than 0.5 MeV and so does the response of the GM detector. Figure 19 illustrates the mass attenuation coefficient for iron, where the difference between 50 and 200 keV is by a factor of around 1000.

In summary, the T2416A GM detector over responds to gamma rays with low energies. For 56 keV, this over response is 80 times higher than its value at 222 keV. The over-response gradually decreases until it reaches an approximately constant energy independent value for gamma rays, with energies starting from 222 keV.

4.1.2 Experimental Results for Bare Detector

To validate the above performed Monte Carlo calculations, a series of experimental investigations were conducted using the T2416A detector. An X-ray machine was used to provide a field of gamma rays with the following energies: 56, 85, 129, 178 and 222 keV. An X-ray machine does not produce beams with a precise energy; rather it produces a beam with a Gaussian distribution of energies around the desired value. In the first set of experiments, four T2416A GM detectors without any filtering material were exposed to a gamma ray field with the above listed energies. The dose rate, measured with the T2416A

GM counters as a function of gamma ray energy, is plotted in Figure 27. The statistical error in the data is an average of four measurements.

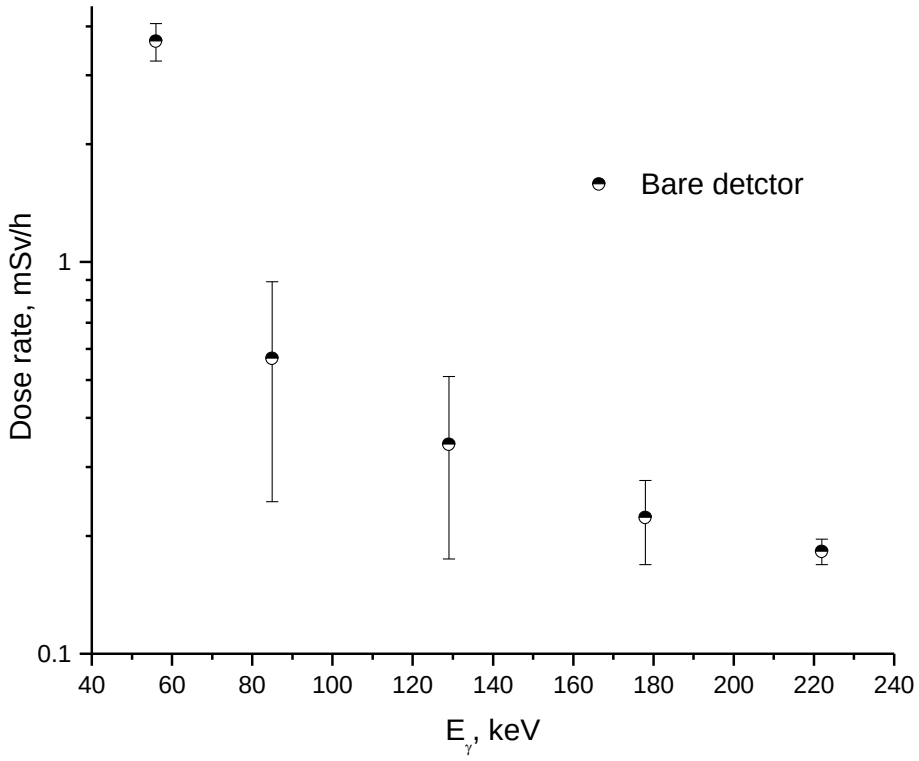

Figure 27: Response Function of the T2416A GM Detector Based on the Experimental Data

The general trend of the response function of the GM detector generated from the experimental work is in good agreement with the simulation results. Figure 28 compares the two sets of data.

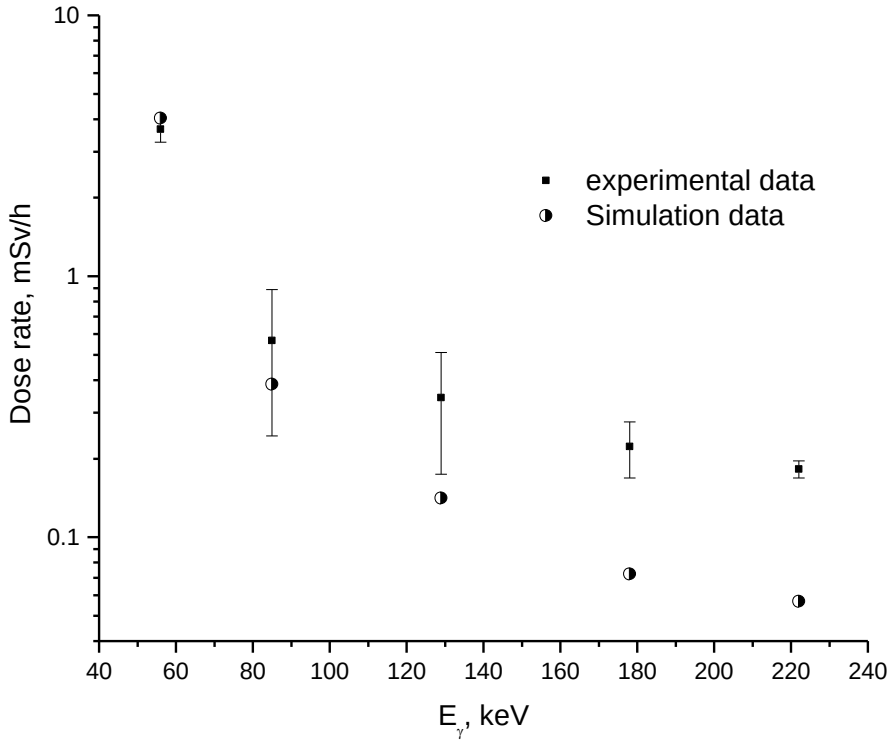

Figure 28: Response Function of the T2416A GM Based on the Experimental and Simulation Data

It is noticed that the over response of the GM detector is slightly higher in the experimental data for energies greater than 120 keV. This difference is attributed to several factors, such as:

- Background contribution in the experiment which was not considered in the simulation.
- In the simulation, mono-energetic gamma rays have been simulated while in the experiment, the X-ray machine offers an average energy (Gaussian distribution of energies)
- The back scattering contribution of the walls, floor and ceiling of the facility was not considered in the simulation.

Both experimental and simulation data illustrate an over response of the T2416A GM detector to gamma rays with energies less than 200 keV. At a later stage of this study, this over response was compensated through the use of an appropriate filtering material wrapped around the detector. In the following sections, two main methods of wrapping the filtering material around the detector are discussed.

4.2 Impact of Wrapping Mechanism on the Response of GM Detector

There are mainly two methods of wrapping the T2416A GM detector: either entire or partial covering of the lateral surface of the detector. The first method is expected to considerably reduce the sensitivity of the counter as it will attenuate gamma rays with energies lower than 50 keV, thereby preventing them from registering counts. This reduction in sensitivity is not as severe with the second method of wrapping. An MCNP/X code was developed to investigate the impact of the two wrapping mechanisms.

4.2.1 Using a One-Piece Wrapping Model

In this model, an MCNP/X code was developed to investigate the use of the one-piece model of wrapping the filtering material. The material used for this investigation was pure tin with a thickness of 80 μm. The data, illustrating the response function of the T2416A GM detector to gamma rays with low energies, using this method in comparison to the response of the bare detector, is presented in Figure 29.

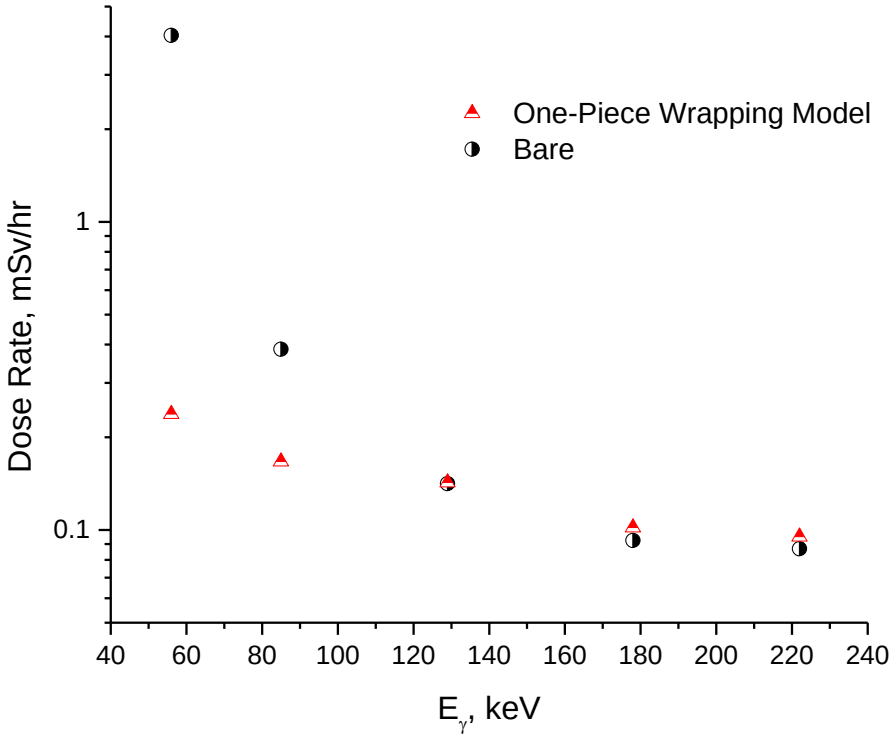

Figure 29: Impact of the One-Piece Wrapping Model Based on MCNPX Modelling

Figure 29 shows that the response of the T2416A GM detector to gamma rays with low energies was moderately reduced when the detector wall was fully covered by the tin filtering material. For instance, the response of the T2416A GM detector, wrapped with lead, to gamma rays with energy of 56 keV was reduced by a factor of 16 relative to the response of the bare detector (see appendix E). Hence, the impact of this wrapping mechanism for gamma rays with energies above 50 keV was positive. However, it has been determined that this method of wrapping would have a negative impact on the response of the T2416A GM detector to gamma rays with energies lower than 50 keV, as illustrated in Appendix E.

4.2.2 Using a Two-Piece Wrapping Model

In this model, two pieces of tin filtering material were used. The main advantage of using this configuration is to allow the detector to detect gamma rays with energies lower than 50 keV.

The width of the gap between the two pieces of filtering material was chosen so that the response of the detector will be as flat as possible without negatively impacting the sensitivity of the counter. Our extensive simulations have shown that having a gap with a width 15% of the total height of the GM detector provides an optimal response. Figure 30 illustrates a 3D view of the T2416A GM detector with the two-piece wrapping model.

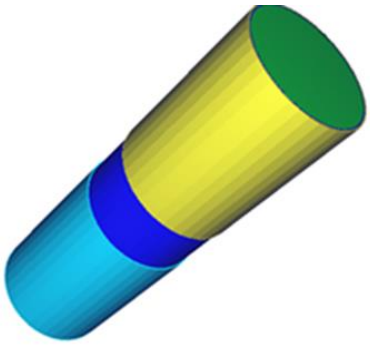

Figure 30: 3D View of the Simulated T2416A Detector with the Two-Piece Wrapping Model

Figure 31 presents the obtained results from the simulation. From this figure, one can see that the response function of the T2416A GM detector with the two-piece wrapping model has a similar response function to the one-piece model in the energy region higher than 50 keV. However, as indicated earlier, the latter model over reduces the response function of

the GM detector to gamma rays with energies lower than 50 keV. Therefore, the two-piece wrapping model has been selected for further investigation.

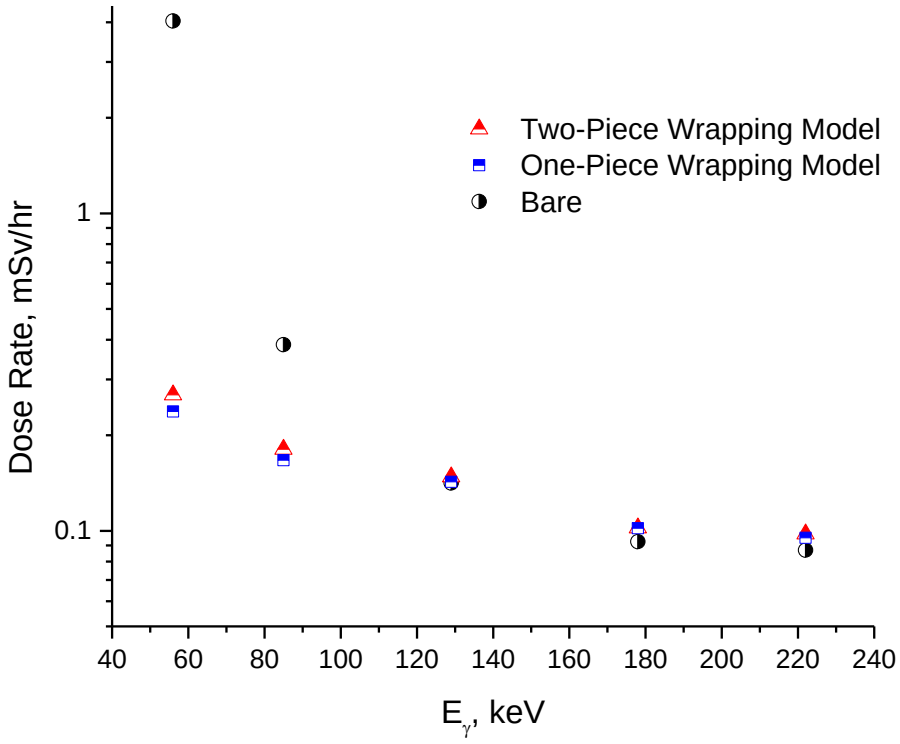

Figure 31: Impact of the Various Wrapping Models

4.3. Response Function of GM Detector Using a Single Filtering Material

Two filtering materials, namely lead and tin, have been selected for this investigation. The impact of each of these two materials on lowering the response function of the T2416A GM detector has been determined and the obtained results are presented and discussed in the following sections.

4.3.1 Response Function of GM Detector Using Lead Filtering Material

Lead is a heavy element with a Z value of 82 and with a high cross section for gamma rays with energies less than 200 keV. Figure 32 compares the linear attenuation coefficient of lead and iron as a function of gamma energy.

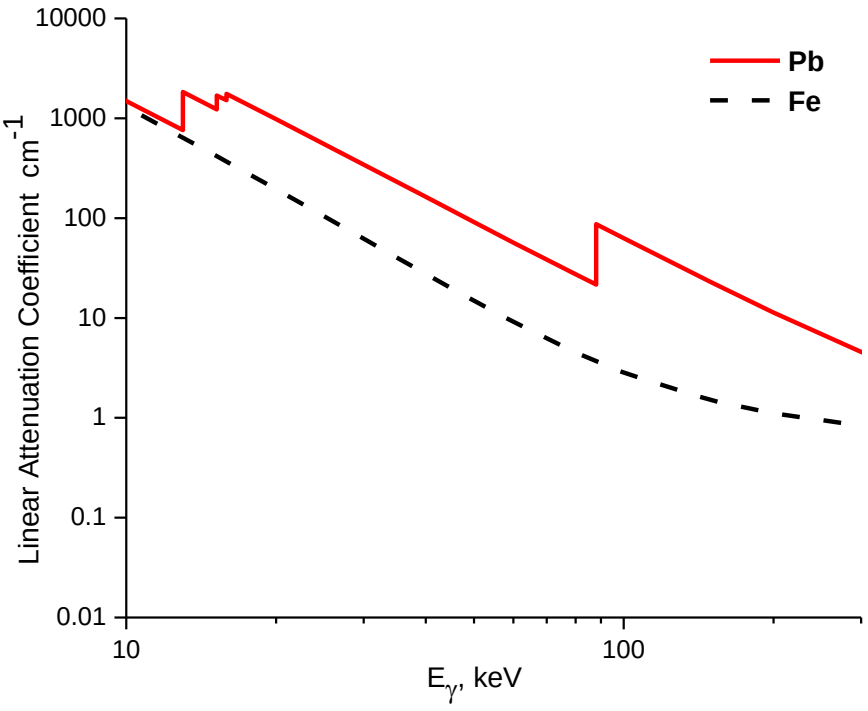

Figure 32: Cross Section of Lead vs. Iron

For gamma rays with low energies, Figure 32 shows that lead has a cross section much higher than iron, which is the main component of the T2416A detector wall. This significant difference can greatly impact the response function of the T2416A GM detector. Lead also has a K absorption edge at 88 keV, which should also impact the response around this energy.

4.3.1.1 Monte Carlo Simulation for the Impact of Lead Filtering Material

In order to determine the impact of the lead filtering material on the response function of the T2416A GM detector, an MCNP/X code was developed to model the response function of the counter when wrapped with different filtering materials. Figure 33 shows the data obtained from MCNP/X carried out with a pure lead filtering material and a bare counter.

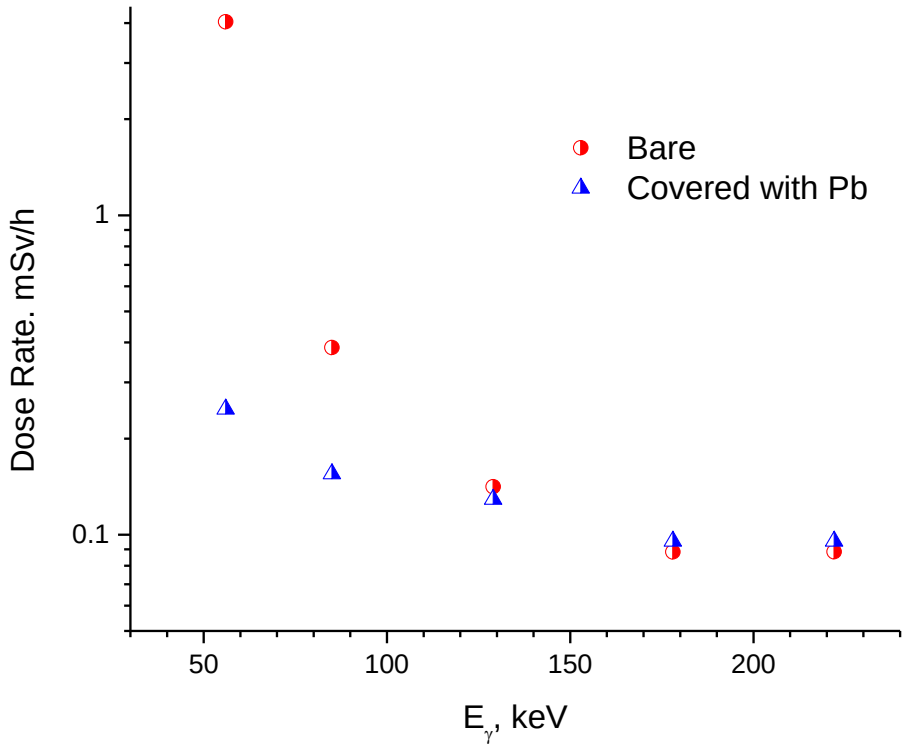

Figure 33: Impact of Lead Filtering Material Based on the Simulation Data

The response of the detector to gamma rays with an energy range from 56 to 130 keV has been significantly reduced. For instance, at 56 keV, the response function has been reduced by a factor of about 16. This reduction is due to the high absorption cross section of lead at this energy. The high cross section ensures that the majority of the incident gamma rays

with this energy interact with the lead filter, and that the ejected photoelectrons that are produced will not be able to enter the gas volume. It should be noticed that, for energies higher than 130 keV, the filtering material does not have a significant impact on the response of the detector due to the significant decrease in the cross section of the filtering material over this range of energies.

It must be noted that, if the response of the detector was calculated for gamma rays with energies around the K absorption edge of lead, a very significant drop in the response would be observed at around 88 keV.

In summary, the lead filtering material has a great impact on lowering the overall response of the T2416A GM detector to gamma rays with energies less than 200 keV. However, it has been determined that the response of the T2416A counter with the lead filtering material was significantly reduced for energies less than 50 keV (see Appendix E).

In addition, as a part of investigating potential filtering materials, different filter thicknesses were investigated. For the initial simulation, the used thickness was 80 μm and, in an attempt to determine the impact of various thicknesses of the lead filtering material to the response of the detector, thicknesses of 30 and 130 μm were also used. Figure 34 compares the data obtained for 30, 80 and 130 μm thicknesses.

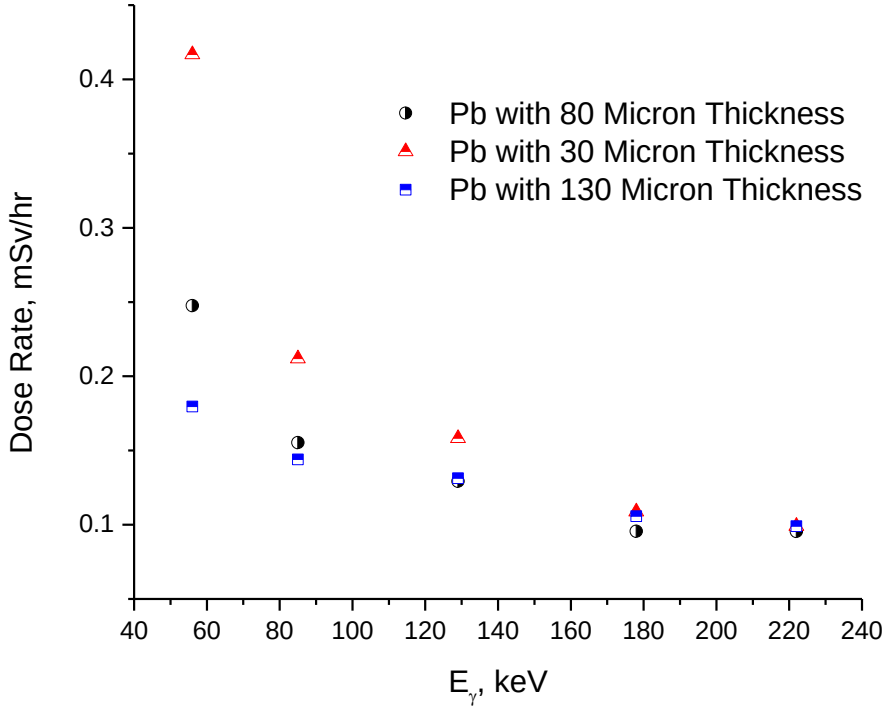

Figure 34: Impact of Lead Filtering material with Different Thicknesses

From Figure 34, it can be noticed that, as the thickness of lead is increased, its impact in lowering the over response is enhanced for gamma rays with an energy range of 56 to 222 keV. However, it was determined from the second set of simulations that increasing the thickness of the lead caused an over reduction in the response function of the detector to gamma rays with energies below 50 keV. This over reduction is undesirable, and hence it was determined that 80 μm was the most ideal thickness.

4.3.1.2 Experimental Results for the Impact of Lead Filtering Material

A total of eight T2416A GM detectors were used in a series of experiments, four of which were wrapped with lead filtering material. The following energies of gamma rays were

selected to irradiate each detector with: 56, 85, 129, 178 and 222 keV. The dose rate with and without filtering was measured as shown in Table 3 and illustrated in Figure 35.

Table 3: Experimental Data with and without Lead Filtering Material

	Dose Rate, mSv/h			
Energy, (keV)	**Bare**	**Statistical Error**	**Covered with lead**	**Statistical Error**
56	3.66	0.40	0.30	0.03
85	0.56	0.32	0.18	0.11
129	0.34	0.17	0.19	0.09
178	0.22	0.05	0.16	0.04
222	0.18	0.01	0.15	0.01

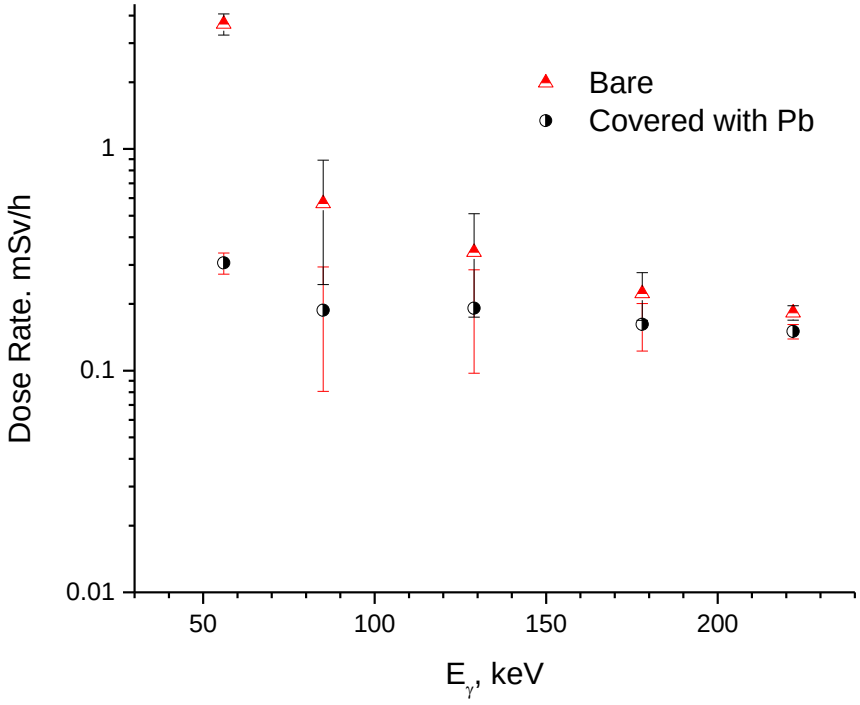

Figure 35: Impact of Lead Filtering Material Based on the Experimental Data

From Figure 35, it can be observed that the lead filtering material was able to reduce the over response of the detector to gamma rays with energies lower than 200 keV. For instance, at 56 keV, the response of the T2416A GM detector was lowered by a factor of 12. Lead filtering material has provided a relatively flat response curve for energies greater than 85 keV.

To compare the experimental data with the simulation, the ratio of the obtained dose rate from both the covered and the bare counters has been calculated. These ratios are shown in Figure 36.

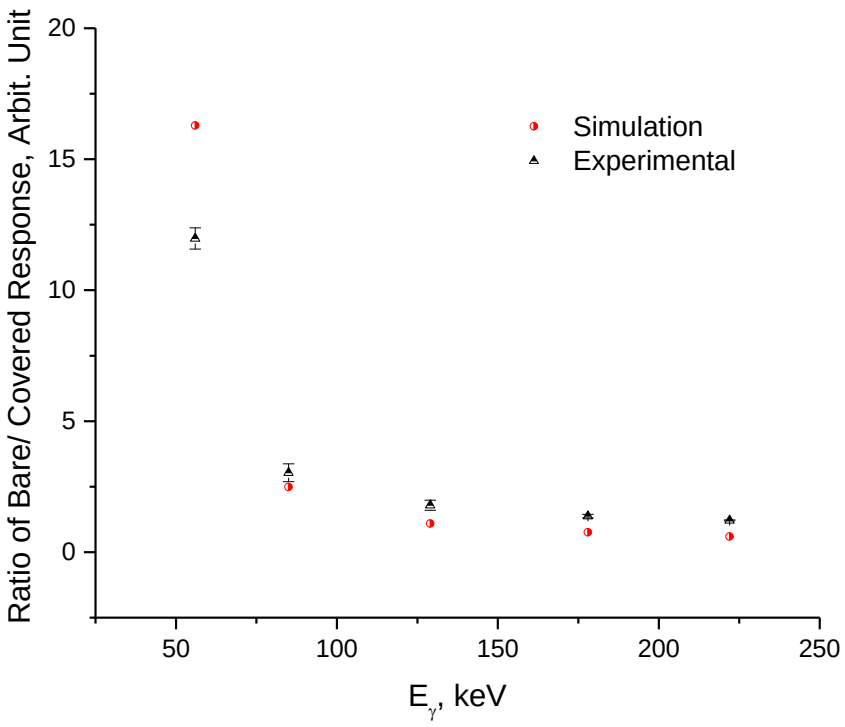

Figure 36: Simulation vs Experimental Data

There is a good agreement between the trend of the simulation and the experimental data. However, the experimental data are slightly higher than the simulation data for energies higher that 85 keV. This difference is attributed to those parameters discussed in section 4.1.2.

4.3.2 GM Detector with Tin Filtering Material

The second filtering material that has been investigated is tin, which has Z=50 and a cross section higher than iron for gamma rays with low energies. Tin also has a K absorption edge that falls around 30 keV. Thus, wrapping the T2416A GM detector with tin filtering material is expected to lower the response of the detector to gamma rays with energies less

than 200 keV with a greater impact around 30 keV. Figure 37 compares the cross section of tin and iron.

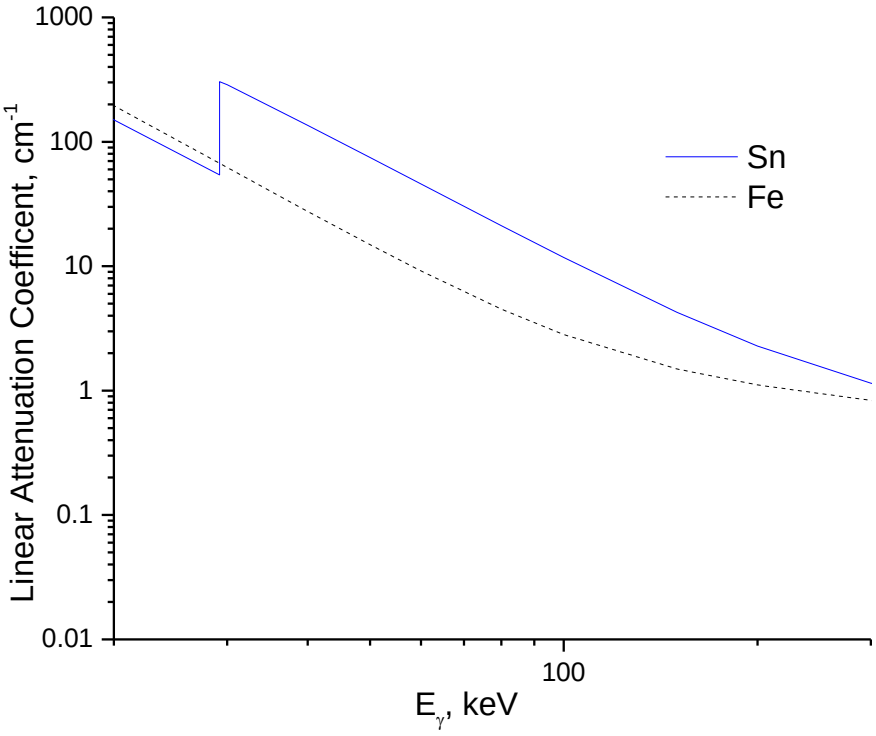

Figure 37: Cross Section of Tin and Iron

4.3.2.1 Monte Carlo Simulation for the Impact of Tin Filtering Material

In order to determine the impact of tin filtering material in lowering the over response of the T2416A GM to gamma rays with energies less than 200 keV, an MCNP model was developed and the obtained results from the simulation are shown in Figure 38. The curves compare the response function of the T2416A GM detector with and without tin filtering material.

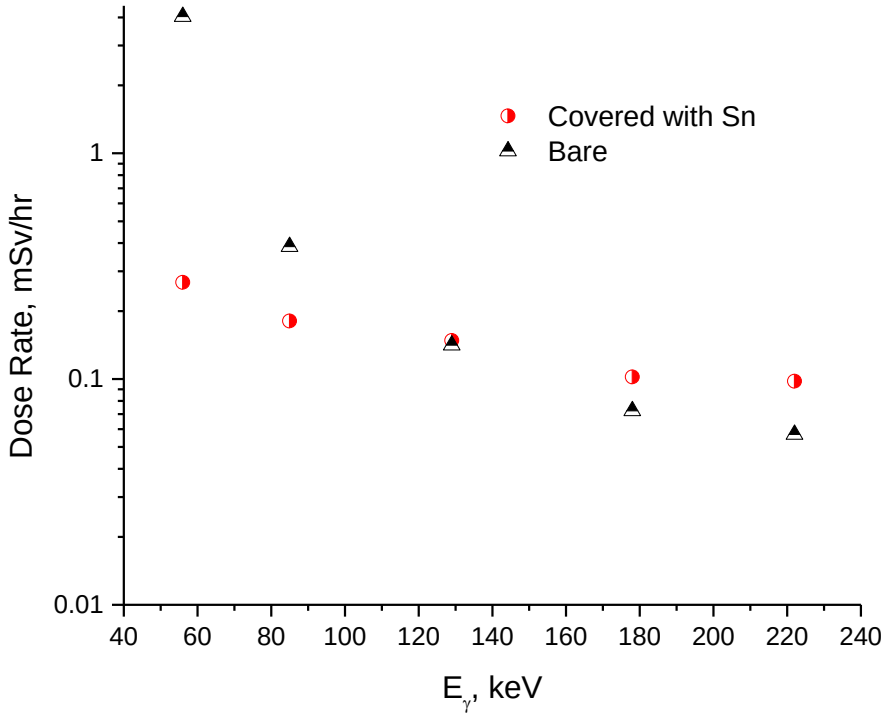

Figure 38: Impact of Tin Filtering Material Based on Simulation

Tin filtering material was able to reduce the over response of the detector to gamma rays with energies less than 200 keV. For gamma rays with 56 keV, the over response was reduced by a factor of 16, compared to 222 keV. This reduction is attributed to the high cross section of tin which is five times higher than that of iron at such a level of energy.

Based on the obtained simulation data, tin filtering material has a great impact on lowering the over response of the detector to gamma rays with energies lower than 250 keV. The response function of the T2416A GM detector has improved by a factor from one to two in the range from 56 to 222 keV. Since tin has an absorption edge at 30 keV, its impact was not determined in this set of data. However, in the second set of simulation data, where

the impact of the filtering material on the response function of the detector for gamma rays with energies less than 50 keV was determined, the impact of the K absorption edge of tin was clearly demonstrated.

Further in the performed calculations, in order to investigate the influence of the thickness, the MCNP/X code was modified to simulate the response of the detector with a different thickness. The initial simulation was performed with a thickness of 80 μm and again two other thicknesses of 30 & 130 μm were selected. Figure 39 compares the response function of the detector with the three thicknesses of tin filtering material.

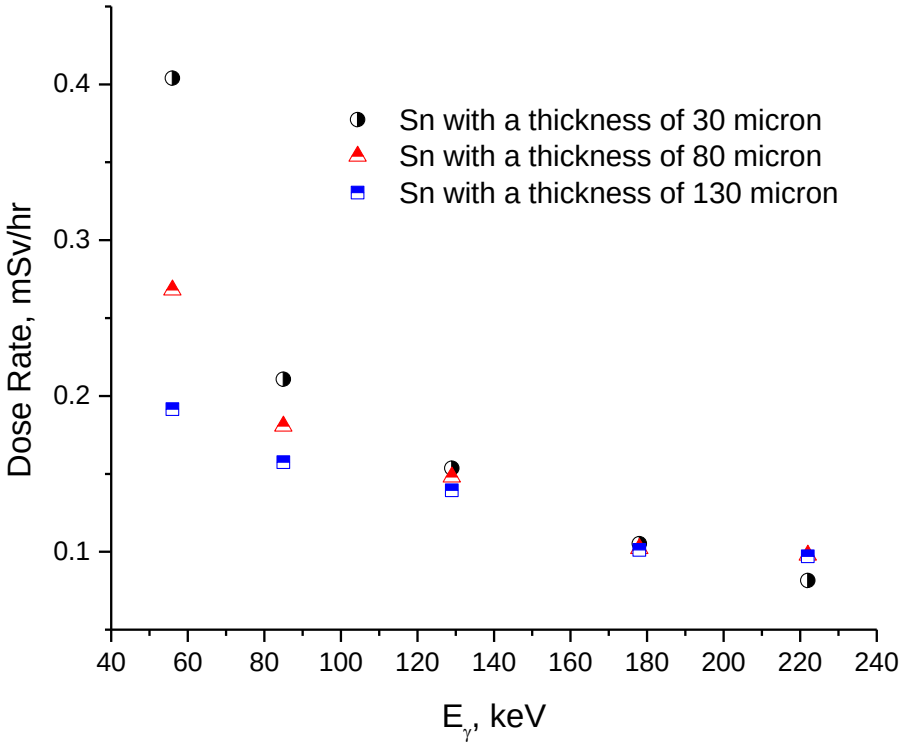

Figure 39: Impact of Tin Filtering Material with Various Thicknesses

As has been seen with the lead filtering material, there is a proportional correlation between the thickness and the degree of lowering the response function of the detector. Generally, the greater the thickness of the filtering material, the greater the impact it has on reducing the over response. Increasing the thickness of the tin filtering material seems to have a positive impact on the response of the detector for gamma rays with energies between 50 and 180 keV; however, this has a negative impact on low energies (less than 50 keV) as illustrated in Appendix E.

Once again, it was determined from the second set of simulations that, by increasing the thickness of the tin filtering material, the K absorption edge had greater impact.

4.3.3 Impact of Tin & Lead Filtering Material

Both lead and tin filtering material have a cross section that are higher than that of iron; hence both materials were able to reduce the over response of the GM detector to gamma rays with energies less than 250 keV. In this section, the effectiveness of using a filtering material, composed of both tin and lead, in lowering the over response of the detector is compared.

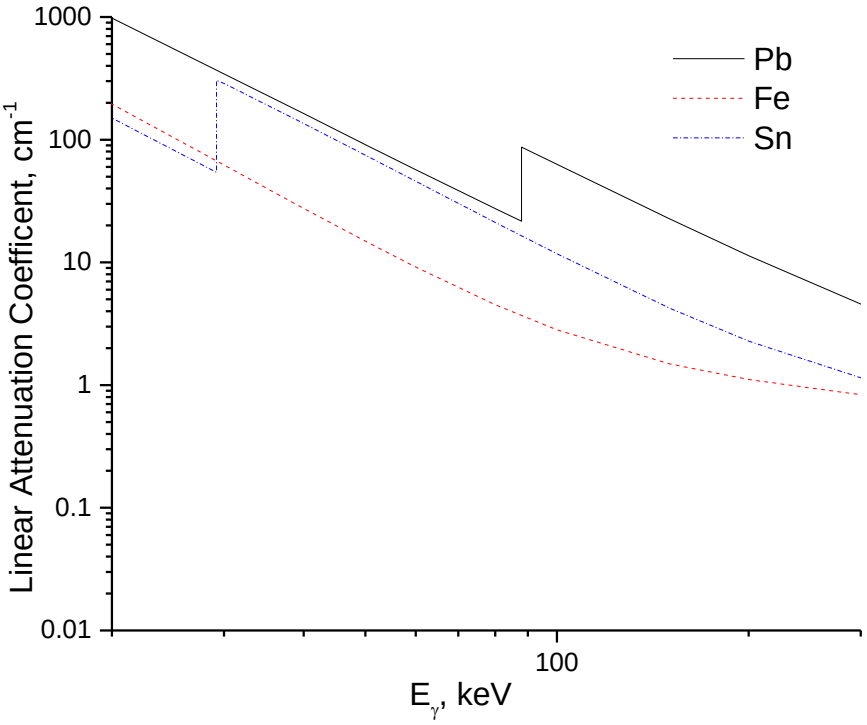

Figure 40: Iron, Lead and Tin Cross Section

Figure 40 shows the cross section for iron, lead and tin. Over the entire energy range shown in Figure 40, iron has the lowest cross section, while lead has the highest. Over the range of 30 to 90 keV, the lead's cross section is very close to that of tin. However, outside this range, from both ends, the cross section of lead is higher than that of tin. Figure 41 compares the response function of the counter when individual lead and tin filters are used.

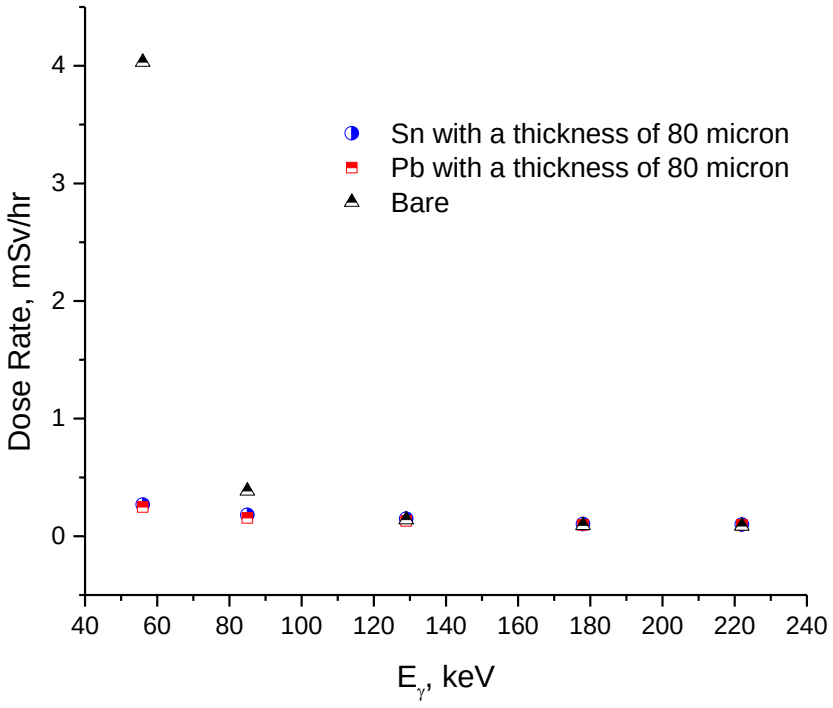

Figure 41: Impact of Tin/Lead Filtering Materials Based on Simulation Data

Figure 41 shows the effectiveness of each of the filtering materials used in lowering the over response of the T2416A GM detector. From 56 to 90 keV, lead has a mass attenuation coefficient that is slightly higher than tin. Hence, both materials have the same impact in lowering the over response of the detector at this range of energies. However, for gamma rays with energies less than 30 keV, lead has a mass attenuation coefficient that is much higher than that of tin. This difference in mass attenuation coefficient is reflected in the ability of lead to drastically lower the response function of the detector at this range of energies, as illustrated in Appendix E. As the energy of the gamma ray increases beyond

90 keV, the ability of both filtering materials to impact the response of the counter is the same.

In the next section, the impact of using a combined filtering material that consists of tin and lead is presented. Similarly, an MCNP/X model has been developed to simulate the response function of the detector with a filtering material containing both tin and lead with various thicknesses and various weighting percentages.

4.4 Impact of Using a Combination of Filtering Materials

From the previous data for tin and lead filtering material as discussed in the preceding section, it was determined that lead had a great impact on lowering the response function of the detector to gamma rays with energies higher than 50 keV. However, lead has a negative impact on the response of the detector for gamma rays with energies less than 50 keV. An in-depth analysis of the cross section in the energy range lower than 50 keV reveals that the tin filtering material provides a better response function for the detector. Therefore, it was decided to use a filtering material that consists mainly of tin, with the addition of a small percentage of lead, to achieve a reasonable response function of the detector.

4.4.1 GM Detector with 70% Tin and 30% Lead

For this combination, the MCNP/X code has been updated to simulate the response function of the detector with a filtering material that contains 70% tin and 30% lead. The obtained result from the simulation is illustrated in Figure 42.

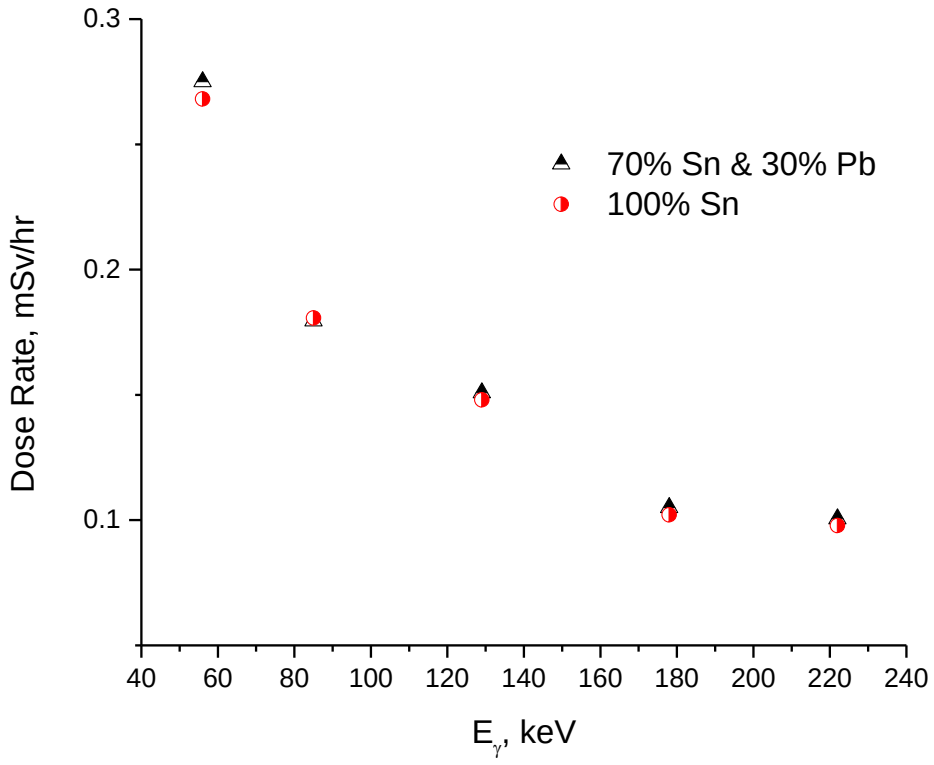

Figure 42: Impact of using a 100% Tin Filtering Material VS. 70% Tin and 30% Lead

Lowering the weight percentage of lead to 30% did not have much of an impact in lowering the response of the detector for gamma rays with energies greater than 50 keV. However, based on the second set of simulations presented in Appendix E, it was determined that using an alloy consisting of lead and tin, with a weight concentration of 30% and 70% respectively, has a negative impact for gamma rays with energies lower than 50 keV. Via the process of trial and error, it was decided to lower the weight percentage of lead in the alloy to 2%.

4.4.2 GM Detector with 98% Tin & 2% Lead Filtering Material

An MCNP/X code was developed to simulate the response function of the T2416A GM detector with a filtering material containing a mixture of tin and lead. A mixture of 98% tin and 2% lead has been used as a filtering material. Due to the lower concentration of lead, the expected response function should be very similar to that with a tin filtering material. However, the impact will be more significant in the energy range lower than 50 keV. The obtained data from the MCNP/X modeling is illustrated in Figure 40, where a comparison between the response obtained from a counter with a pure tin filter, and that from a counter with a filter composed of 98% tin and 2% lead, is presented.

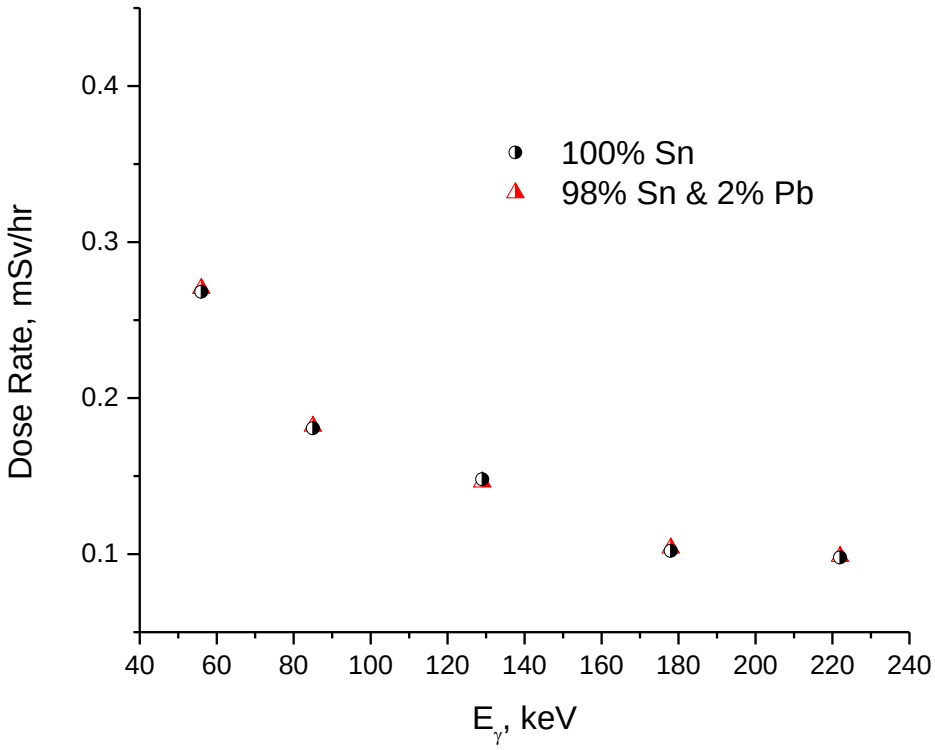

Figure 40: Impact of 98% Tin and 2% Lead Filtering Material

As predicted, the addition of the 2% lead did not have much impact on the response of the detector to gamma rays with energies greater than 50 keV. However, from the MCNP calculations, presented in Appendix E, it was confirmed that having a 2% lead concentration mixed with 98% tin has a positive impact in bringing the response function of the GM detector to an acceptable level of flatness for gamma rays with energies less than 50 keV.

Further adjustment of the MCNP/X code was performed to investigate the impact of various thicknesses on the response function of the detector while keeping the same

material combination of 2% lead and 98% tin. Three thicknesses have been used, namely 30 μm, 80 μm and 130 μm. The obtained data are shown in Figure 43.

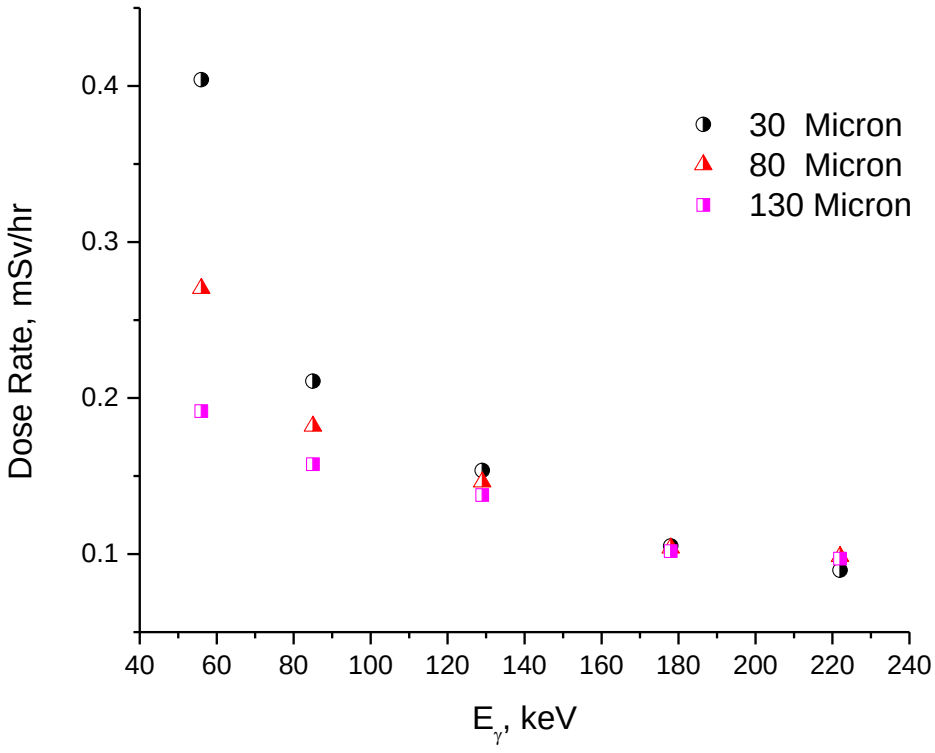

Figure 43: Impact of 98% Tin and 2% Lead Filter with Various Thicknesses Based on MCNPX Modelling

Increasing the thickness of the filtering material to 130 μm lowered the response function of the detector to gamma rays with energies from 50 to 180 keV. However, such an impact was not observed for higher energies. As in previous cases, due to the higher cross section in the energy region lower than 50 keV, the impact on lowering the response function was significant. A separate investigation was conducted for such energies; the results showed an over reduction of the response which makes the detector almost insensitive to gamma rays with low energies. Consequently, it was decided to employ a thickness of 80 μm that

offers a response of around $\pm$36 % for the energy region between 56 and 222 keV and $\pm$25% for energies lower than 50 keV.

Conclusion

In collaboration with UOIT and Canberra Co., a project was initiated in 2011 to transform a world-wide employed Geiger Muller detector to be an energy compensated GM detector.

In this work, Monte Carlo models were built to simulate the response function of the T2416A GM counter in different configuration and geometries. The performed calculations with a MCNP/X model were validated through a series of experimental investigations using the T2416A GM detector from 56 to 222 keV.

The investigation includes two main design features: the wrapping mechanism and the use of different filtering materials, namely, lead and tin, and a combination of both with different thickness and weight percentages.

The first design feature to be investigated was the wrapping mechanism, of which mainly two were investigated, using a one-piece wrapping model that covers the lateral surface of the detector and a two-piece wrapping model that partially covers the lateral surface of the T2416A GM detector. The T2416A GM detector with the latter method of wrapping seems to have a better response function than the one-piece wrapping model, especially for gamma rays with low energies.

The second design feature that was examined is the use of an appropriate filtering material. Two types of filtering materials were used: a single and a combination of filtering materials.

For the single filtering material, both lead and tin were investigated with regard to their ability to provide the T2416A GM detector with a reasonable response function. It has been observed that tin filtering material is more effective in lowering the over response of the detector to gamma rays over a wider range of energies. The most appropriate thickness of tin filtering material was 80 μm. Lead was also able to reduce the response of the detector, but only over a specific range of gamma energies; i.e. greater than 50 keV.

In the second part of investigating into the use of an appropriate filtering material, a combination of lead and tin were used in various weight percentages and thicknesses. Wrapping the detector with a 98% tin and 2% lead with a thickness of 80 μm produced the optimal response function for gamma rays with a wide range of energies.

Finally, 80 μm thick filtering material, consisting of 98% tin and 2% lead, wrapped using the two-piece model has been adopted for further development of the counter.

Future work

Future work to further investigate the impact of the filtering materials on the response function of the T2416A GM detector as well as investigations on the polar response of the detector (angular dependence) should be conducted. Additional investigation can be done to determine the impact of other wrapping mechanisms such as a multi-gap system or the use of spiral strips. Illustrations of some alternative wrapping mechanisms are provided in Appendix D. Performing further experimental work to validate more of the simulation results would be a great asset to this work.

REFERENCES

[1] P. W. Frame, "A History of Radiation Detection Instrumentation," *Health Physics,* vol. 87, no. 2, p. 623, 2004.

[2] G. Knoll, Radiation Detection and Measurement, 11-15, 49-53, 310-353: John Wiley & Sons, 2000.

[3] C. Herman, Introduction to Health Physics, 75-84, 119-136, 343-355: McGaw-Hill, 1996, pp. 75-84, 119-136, 343-355.

[4] D. Barclay, "Improved Response of Geiger Muller Detectors," *IEEE Transactions on Nuclear Science,* vol. 33, no. 1, pp. 613-616, 1986.

[5] J. E. Turner, Atoms, Radiation and Radiation Protection, 68-78, 173-187, 241-266: Wiley, 2007, pp. 68-78, 173-187, 241-266.

[6] C. R., "Hyper Physics," Georgia State University , [Online]. Available: http://hyperphysics.phy-astr.gsu.edu/hbase/quantum/xrayc.html. [Accessed 07 January 2012].

[7] G. Nelsom D. Reolly, "Gamma Interactions," in *Passive Nondestructive Assay of Nuclear Material*, Los Alamos, U.S. Goverment Printing Office, 1991, pp. 27-42.

[8] U.S. Department of Energy , "DOE Fundamentals Handbook Instrumentations and Control," National Technical Information Service, Washington, D.C., 1992.

[9] Smith, Hastings; Marcia, Lucas, "Gamma Ray Detectors," in *Passive Nondestructive Assay of Nuclear Materials*, Washington, DC, U.S.Government Printing Office, 1991, pp. 43-63.

[10] Canberra, "Gamma and X-Ray Detection," Canberra Industries, Meriden, 2010.

[11] "National Institute of Standards and Technology," National Institute of Standards and Technology, [Online]. Available: http://www.nist.gov/index.html. [Accessed 12 January 2013].

[12] "Geiger Muller Tubes," Centronic , [Online]. Available: http://www.centronic.co.uk/. [Accessed 1 January 2010].

[13] S. Ahmed, Physics and Engineering of Raiation Detection, Academic Press Inc., 2007.

[14] P. Burgess, "Determination of the Suitability of Energy Compensated GM Tube for The Measurement of X Radiation Transmitted Through Shielding," *Radiation Protection Dosimetry,* vol. 16, no. 3, pp. 243-246, 1986.

[15] J. K. Shultis and R. E. Faw, "AN MCNP PRIMER," Dept. of Mechanical and Nuclear Engineering, Manhattan, KS 66506, Rev 2005.

[16] J. E. Turner, "Interaction of Ionizing Radiation with Matter," *Health Physics,* pp. 520-543, 2005.

[17] "Canberra Co.," Canberra Co., [Online]. Available: http://www.canberra.com/products/hp_radioprotection/csp-survey-meters.asp. [Accessed 1 March 2013].

[18] Boxue Liu, Yanchum Wang, Bo Xie, Hao Zhang, "Calculation of Energy Response of Cylindrical G-M Tubes with EGS4 Monte Code," *IHEP,* vol. 5, no. 006, pp. 1-5, 2001.

[19] Vitaly Danchenkot, Nicolas Mitrofanov, "Chlorine-Neon Geiger-Muller Counters with Energy-Independent Gamma Ray Efficiency," *Review of Scientific Instruments,* vol. 35, pp. 1076-1077, 1964.

[20] X-5 Monte Carlo Team, "MCNP-A General Monte Carlo N-Particle Transport Code," Los Alamos National Laboratory, Oak Ridge, 2008.

[21] F. Flakus, "Detecting and Measuring Ionizing Radiation - A Short History," *IAEA,* vol. 23, no. 4, pp. 31-36, 1981.

[22] D. Wilkinson, "The Geiger Discharge Revisited Part 1. The Charge Genrated," *Nuclear Instruments and Methods in Physics Research Section A,* vol. 321, no. 1-2, pp. 195-210, 1992.

[23] D. Wilkinson, "The Geiger Discharge Revisited Part 4. The Fast Component," *Nuclear Instruments and Methods in Physics Research Section A,* vol. 435, no. 3, pp. 446-455, 1999.

[24] D. Wilkinson, "The Geiger Discharge Revisiting Part 3. Convergence," *Nuclear Instruments and Methods in Physics Research Section A,* vol. 383, pp. 523-527, 1996.

Appendices

Appendix A: MCNP/X Code

```
c ESNS-11-001  Geiger counter: spectral gamma sensitivity.
c Data: January 19, 2011
c Geometry: Cylinder from Fe-Cr and gas inside.
c  Geiger detector from Canberra: Model 2416.
c Task: Detector sensitivity: counts vs. gamma energy.
c
c -------------------------------------------------------------
c cell cards
   1    11 -0.0058 -1  $ gas
   2    22    -7.6 1 -2  $ Fe-Cr camera
  ====================================
  ====== Removed Intentionally =========
 ====================================
   6    0        6 -7
   7    0        7  $ outside of my interest


c -------------------------------------------------------------
c surface cards
   1      rcc 0 0 -1.5 0 0 3 0.448579
   2      rcc 0 0 -1.5 0 0 3 0.457
  ====================================
  ====== Removed Intentionally =========
 ====================================
   6      rcc 0 0 -1.5 0 0 3 0.47
   7      rpp -0.5 0.5 -3 0.5 -1.6 1.6
```

```
c Mode
mode  p e
c material card
  ===================================
  ====== Removed Intentionally =========
 ===================================
    24000.           -0.3
m33   50000.            0.7  $ Pb
    82000.           0.3
imp:p   1 5r       0          $ 1, 7
imp:e   1 5r       0          $ 1, 7
c source card
sdef  PAR= 2 ERG= 0.029 POS= 0 -3 0 X=D1 Y=-3 Z=D2 $
  ===================================
  ====== Removed Intentionally =========
 ===================================
sp2  0 1
f111:e 1.1
c111 0 1
e111 0 1e-10 1e-9 1e-8 1e-7 1e-6 1e-5 1e-4 1e-3 1e-2 .1 1 10
c
  ===================================
  ====== Removed Intentionally =========
  ===================================
stop NPS 2e+9 CTME 7 $ F111 0.0
c --------   END of PROGRAM   ----------------------
c ------------------------------------------------------------
```

Appendix B: Experimental Data

Bare detector

Enegy kev/ Tube #	Tube 1 (mSv/hr)	Tube 2 (mSv/hr)	Tube 3 (mSv/hr)	Tube 4 (mSv/hr)	Average (mSv/hr)
56	3.57	3.67	3.66	3.76	3.6
85	0.55	0.58	0.57	0.57	0.56
129	0.35	0.36	0.29	0.36	0.34
178	0.21	0.22	0.22	0.22	0.22
222	0.18	0.18	0.18	0.18	0.18

Detector wrapped with lead filtering material

Enegy kev/ Tube #	Tube 1 (mSv/hr)	Tube 2 (mSv/hr)	Tube 3 (mSv/hr)	Tube 4 (mSv/hr)	Average (mSv/hr)
56		0.3	0.31	0.30	0.30
85	0.20	0.18	0.18	0.181	0.18
129	0.21	0.18	0.17	0.193	0.19
178	0.16	0.16	0.15	0.16	0.16
222	0.15	0.14	0.15	0.15	0.15

Appendix C: T2416A Spec. Sheet (Courtesy Canberra Co.)

CANBERRA

GM Miniature Detectors

Features

- Rugged construction designed to tolerate harsh operating conditions
- Halogen quenched to maximize operating life
- A wide range of sensitivities to suit customer needs
- Ideal for small monitoring equipment and personal health physics applications
- Low cost and very reliable over long periods of time

- **Our Warranty:** CANBERRA warrants that its Geiger Mueller detectors will be free from defects in materials and workmanship for a period of one (1) year from the date of initial shipment.

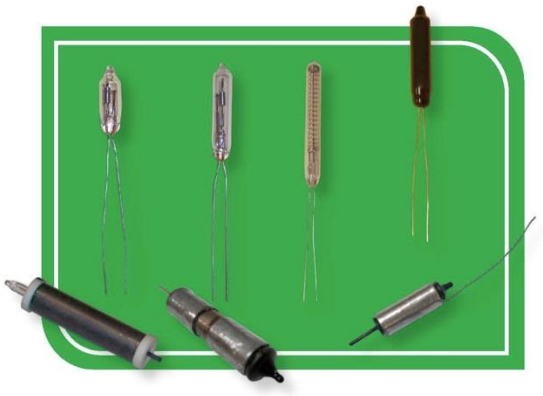

Description

The range of our Miniature GM Detectors offers a wide choice of sensitivity levels available to meet our customer requirements. From low level background environments to levels up to 1000 R/hr. gives our customer the opportunity to select the ideal detector for their application.

Robust construction and the ability to withstand excessive shock and vibration as required for military applications, makes these detectors an ideal choice for small hand held pocket dosimeters and small portable health physics monitors. Please contact us should you wish to discuss specific requirements or references.

GM Miniature Detectors

Gamma Sensitive Miniature Detectors

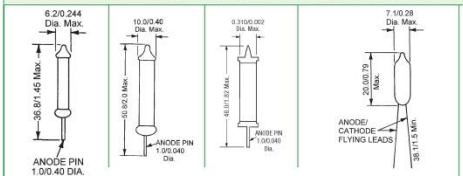

Anode pin connector and cathode strap are supplied. Stated wall thickness includes glass envelope and cathode wall where appropriate. To achieve maximum linear count rate, always solder Ra directly to the supplied anode pin connector, or to the anode flying lead.

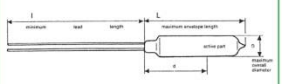

L – Max. Length without Leads

D – Max. Overall Diameter

Detector Type → Characteristics ↓	T2411M	T2416A	T2417A	T2420M	T2422	3G70/ EM14752 3G70	4G60M/ EM14754 4G60M	4G2500/ EM14749 4G2500	3G6500/ EM14748 3G6500
Sensitivity*** ^{137}Cs cpm at 1 mR/h*	84	420	450	4.2	0.66	4.2	4.2	150	270
Window Area Density (mg/cm^2)	N/A	N/A	N/A	N/A	N/A	N/A	N/A	N/A	N/A
Window Effective Diameter (mm, in.)	N/A	N/A	N/A	N/A	N/A	N/A	N/A	N/A	N/A
Recommended Operating Voltage (HV+)	575	575	575	500	460	460	500	550	460
Plateau Length Volts min.	500–650	500–650	500-650	450–550	450–550	420–500	450–550	500–600	420–500
Plateau Slope (%100 V max.)	15	8	8	35	40 max.	30	30	25	25
Dead Time (µs max.)	15	45	45	20	10	25	25	35	50
Background (cpm)*** Shielding 2" Pb + 1/8" Al	2 max.	12 max.	5 max.	6 typ.	0.6 typ.	0.6 max.	0.6 max.	6 max.	10 max.
Test Circuit	Figure 2	Figure 2	Figure 2	Figure 2	Figure 2	Figure 2	Figure 2	Figure 2	Figure 2
Resistor Ra (MΩ)	2.2	4.7	4.7	4.7	4.7	4.7	4.7	4.7	4.7
Operating Temp. (°C)	–40 to +75	–40 to +75	–40 to +75	–51 to +71	–20 to +60	–20 to +60	–20 to +60	–20 to +60	–20 to +60
Cathode Material	Cr/Fe	Cr/Fe	Cr/Fe	Cr/Fe	Cr/Fe	Cr/Fe	Cr/Fe	Cr/Fe	Cr/Fe
Cathode Wall	80–100 mg/cm^2	64–80 mg/cm^2	64–80 mg/cm^2	360–400 mg/cm^2	360–400 mg/cm^2	360 mg/cm^2	360 mg/cm^2	260 mg/cm^2	280 mg/cm^2
Max. Overall Length including Pins (mm, in.)	37, 1.46	51, 2.0	46, 1.82	20, 0.8	20, 0.8	34, 2.91	20, 2.36	34, 2.91	54, 3.7
Max. Overall Diameter (mm, in.)	6.2, 0.244	10, 0.4	9.20, 0.36	7, 0.28	7, 0.28	7, 0.28	7, 0.28	7, 0.28	7, 0.28
Window Recess (mm, in.)	N/A	N/A	N/A	N/A	N/A	N/A	N/A	N/A	N/A

*An exposure of 115.07 mR in air equates to 1.0 mGy. ***At recommended operating voltage.

The T2422 detector is equivalent to the 3G10.

GM Miniature Detectors

Test Circuits
For HV and R_a values see chart.

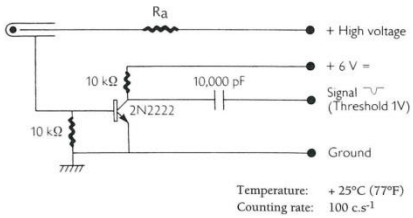

Figure 2 – Cathode Output

Plateau Calculations
Plateau slope calculations for CANBERRA data sheets are based upon IEC recommended formulae, as prescribed in the ISO affiliated publication #151-25 part 25, "Methods of measurement of Geiger Mueller counter detectors".

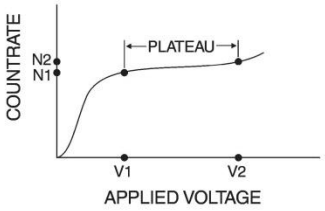

$$\frac{N2-N1}{1/2(N1+N2)} \times \frac{100}{V1-V2} = \%\ \text{per volt}$$

Dead Time Correction
GM detectors using conventional counting circuitry all exhibit counting losses due to the Dead Time factor. These factors cited in the CANBERRA detector data tables are based on the recommended operating voltages and test circuits. The chart below enables the user to estimate the counting losses due to the Dead Time factor at high count rates.

$$\frac{n}{m} = \frac{1}{1-m\tau}$$

n = "True" Counting Rate
m = measured Counting Rate
τ = Dead Time (microseconds)

GM Miniature Detectors

	CANBERRA	Centronics	LND	Saint Gobain
Miniature Detectors	T2411	ZP1310	714	N116-1/C1310

APPLICATIONS

Detector Type	Applications
T2411	Dosimeters
T2411M	Military
T2416A	Dosimeters, Small Portable Monitors
T2417A	Dosimeters, Small Portable Monitors, Military
T2420M	Military
T2422	Dosimeters, Small Portable Monitors

Specifications

ORDERING INFORMATION

- 48258 – T2411M.
- 48185 – T2416A.
- 48162 – T2417A.
- T2420M – T2420M.
- T2422 – T2422.
- EM14752 – 3G70.
- EM14754 – 4G60M.
- EM14749 – 4G2500.
- EM14748 – 3G6500.

OPTIONS

- T2416A/Sv – Sievert Units Energy Shield Fitted.
- T2417A/Sv – Sievert Units Energy Shield Fitted.
- T2417A/Gy – Gray Units Energy Shield Fitted.

ISO 9001 SYSTEM CERTIFIED

Appendix D: Alternative Wrapping Mechanism

The following alternative of wrapping mechanism has the entire lateral surface covered with equal size holes in different areas. The total area of these holes equals to the gap width in the two-piece model wrapping mechanism.

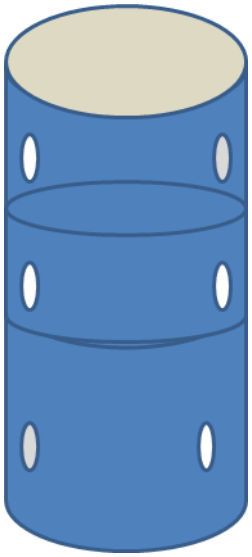

Appendix E: Second Set of Simulation Data for Energies lower than 50keV

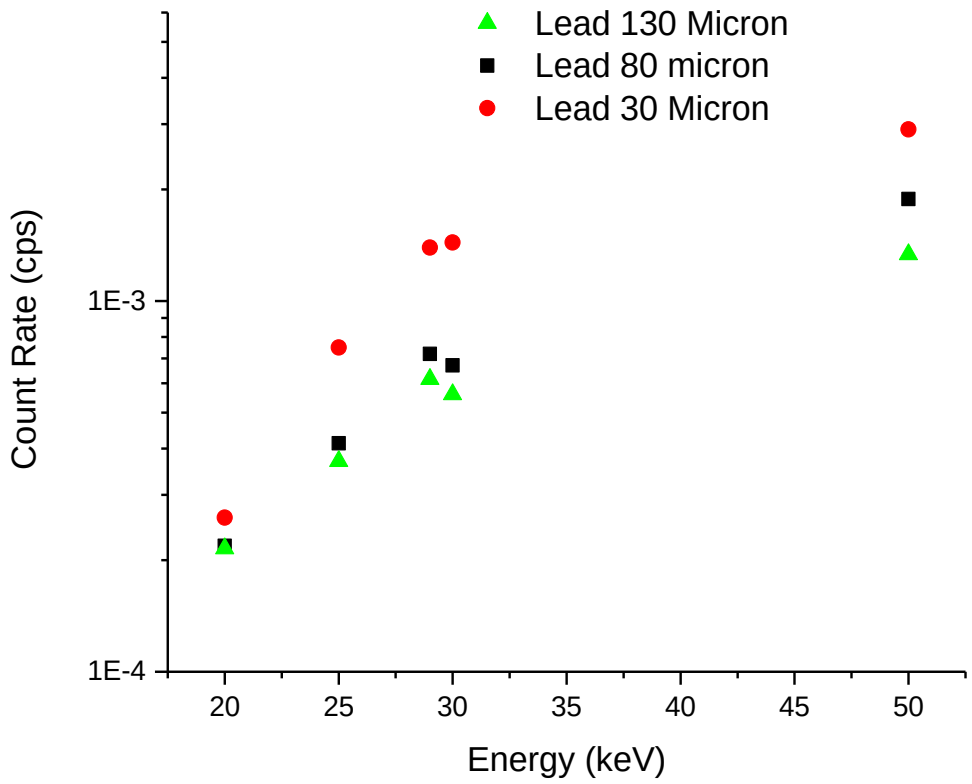

Impact of different thicknesses of lead in the response function of the T2416A GM detector

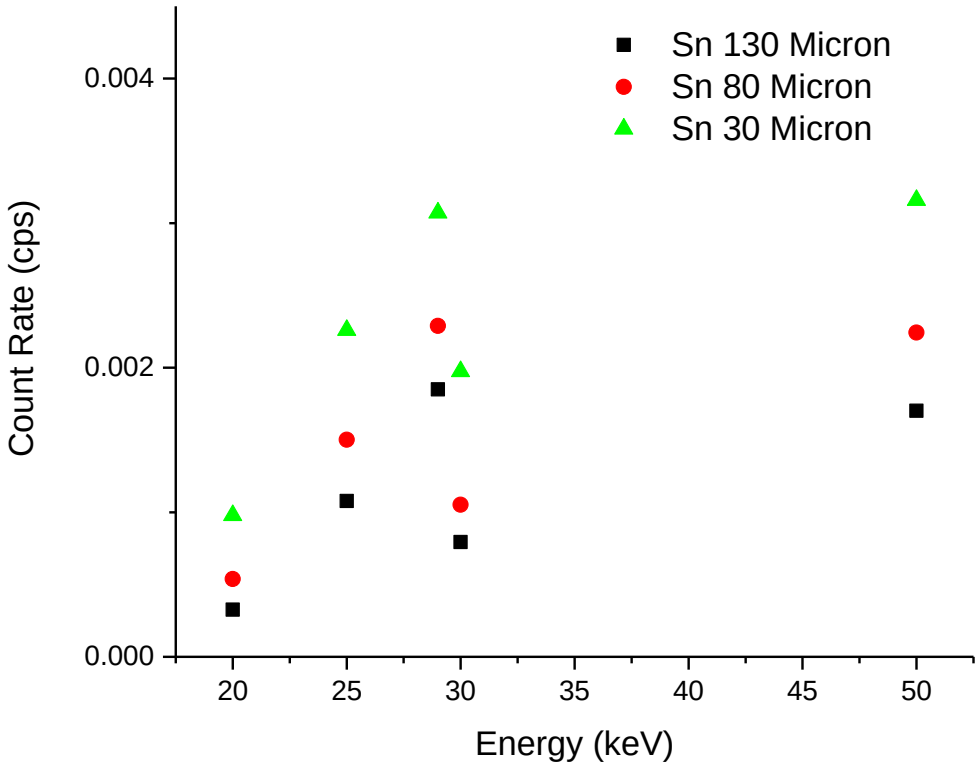

Impact of different thicknesses of tin in the response function of the T2416A GM detector

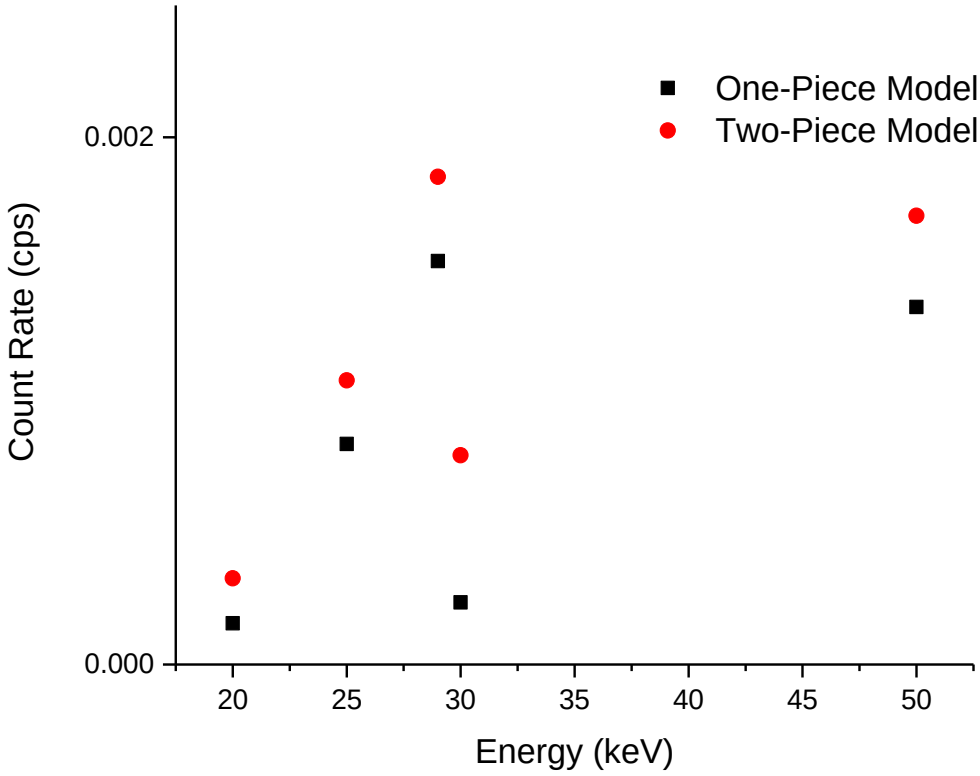

Impact of wrapping mechanism on the response function of the T2416A GM detector

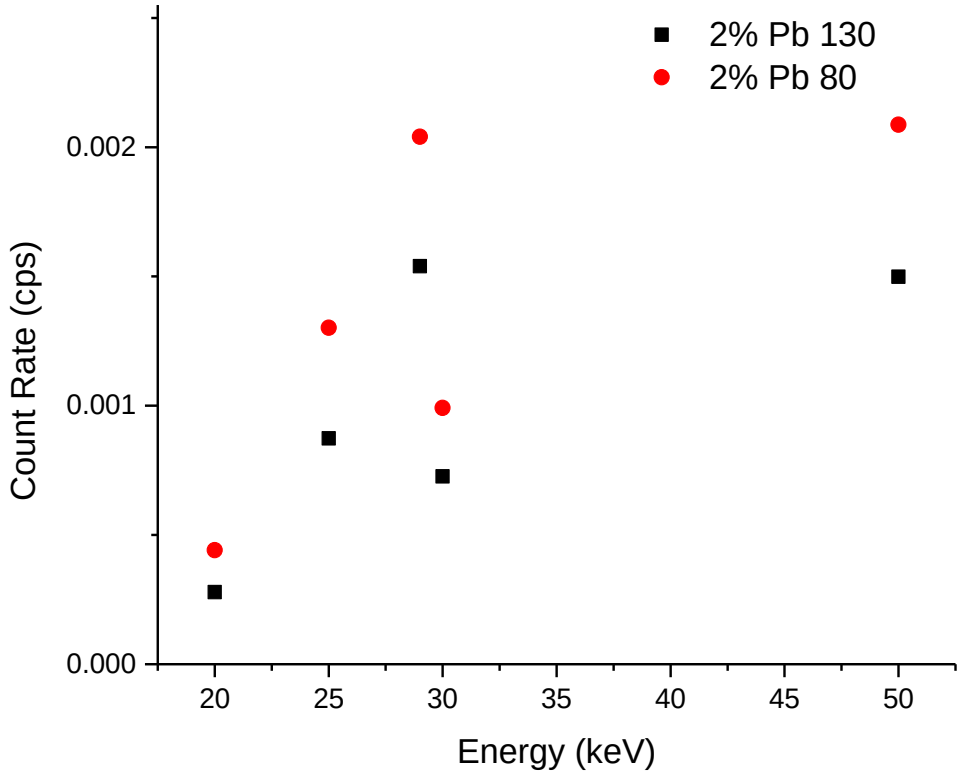

Impact of different thicknesses of 98% tin and 2% lead in the response function of the T2416A GM detector

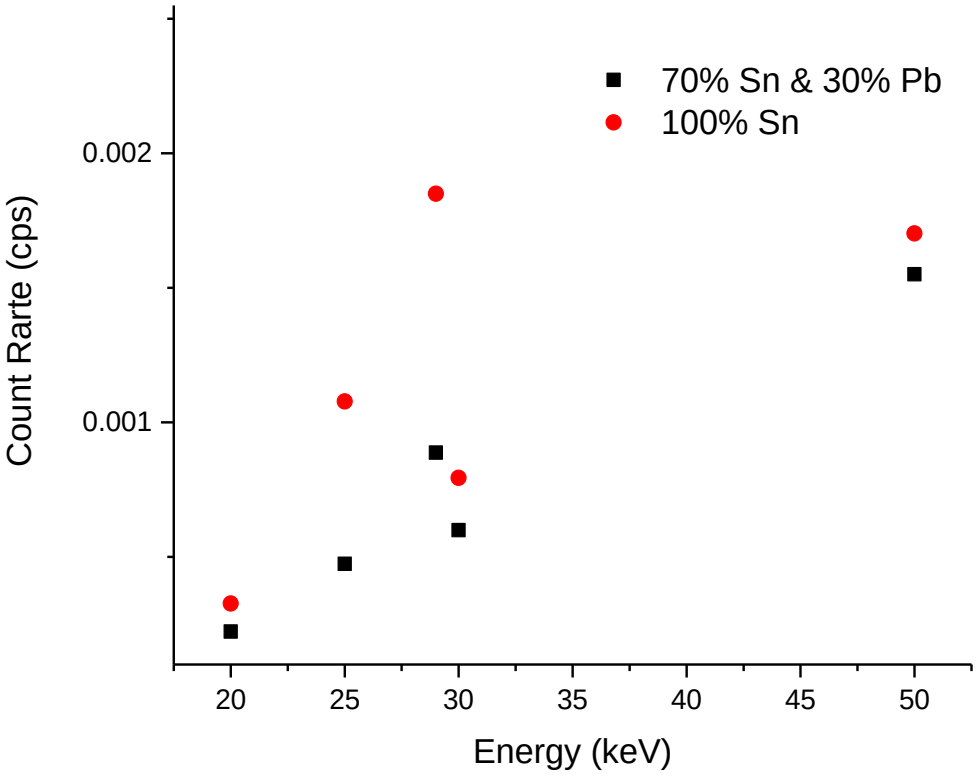

Impact of 70% tin and 30 % lead in the response function of the T2416A GM detector